Analysis of optimal liquidation in limit order books for portfolios of correlated assets with stochastic volatility

Blair, James W. and Johnson, Paul V. and Duck, Peter W.

2015

MIMS EPrint: **2015.49**

Manchester Institute for Mathematical Sciences
School of Mathematics

The University of Manchester

ISSN 1749-9097

Analysis of optimal liquidation in limit order books for portfolios of correlated assets with stochastic volatility

James W. Blair, Paul V. Johnson, & Peter W. Duck*

Abstract

In this paper we study optimal liquidation under two settings: the first being for a basket of correlated assets, the second being for a portfolio of a single asset but under a stochastic volatility model. Under both frameworks we use a combined approach of accurate numerical methods and asymptotic analysis to investigate and gain insight into the solution, with each approach informing and confirming the other. We are able to make a significant improvement in efficiency in both problems, reducing the resulting Hamiliton-Jacobi-Bellman (HJB) partial differential equations (PDEs) to classical non-linear PDEs, as well as reducing the number of variables and input parameters, the latter through non-dimensionalisation. We present numerical solutions to both problems, before further investigating the solution topology through the use of asymptotic analysis in various limits. In some cases we are able to find analytic approximations for both the value function and indeed the optimal liquidation strategies. Furthermore, the solutions we present are comparable with those of Markowitz Portfolio Theory (MPT) for the multiple-asset case, and to those of option pricing theory under stochastic volatility for the stochastic volatility model. For the former we find the trader trades in a way that results in a diversified portfolio, while for the latter we find that more noise in the volatility can be beneficial for the trader in certain regimes, despite being risk-averse.

Optimal liquidation; Asymptotic analysis; Stochastic optimal control; Algorithmic trading; High-frequency trading; Heston volatility model; Stochastic volatility; Portfolio liquidation

1 Introduction

Optimal liquidation has the aim of selling or buying a portfolio of assets over generally a specified time, while minimising the cost to the trader. In the late nineties, the impact of these execution costs was examined by Bertsimas et al. (1999) while simultaneously being studied by Almgren and Chriss (1999, 2001). This is often referred to as the Almgren & Chriss framework, and involves examining the optimal liquidation of a portfolio of an asset before some specified terminal time in which liquidation incurs some market impact, both instantaneously (execution cost) and permanent. The objective was to find the optimal rate of trading which maximised a mean-variance function, with the asset price following a standard Brownian motion.

In the original setting the impact functions were linear. This was extended to non-linear impact functions in Almgren (2003). Schied and Schöneborn (2007) extended to optimising the utility function of an investor with constant-absolute-risk-aversion (CARA) and Schied and Schöneborn (2009) further extended the model to general utility functions. Forsyth et al. (2012) used numerical methods to examine the problem under a Geometric Brownian Motion (GBM) for the asset price. Ten years after the original framework, the problem was extended to include stochastic liquidity and stochastic volatility (Almgren, 2009, 2012). In the original framework it was assumed that a trader was liquidating a quantity of a single asset, so only a single price

*School of Mathematics, The University of Manchester, M13 9PL Manchester, UK (email: jblair@ma.man.ac.uk, pjohnson@ma.man.ac.uk, duck@ma.man.ac.uk).

process was present. Schied et al. (2010) extended this framework to liquidation of a basket of correlated assets, under a CARA utility function, which were found to have deterministic strategies.

The use of temporary market impact did not take the resilience of the order book into consideration. Obizhaeva and Wang (2013) introduced a transient market impact, replacing the instantaneous market impact of Almgren & Chriss. This linear impact is a decaying function of time, representing the resilience of the Limit Order Book (LOB). Alfonsi et al. (2010) extended for general shape functions for the LOB. Kharroubi and Pham (2010) included discrete time trading but in a continuous clock by introducing a lag variable. Numerical methods (finite-differences) for this problem were discussed in Guilbaud et al. (2010). For a more indepth discussion in this area see the review paper of Schied and Slynko (2011).

The above literature focuses on liquidity consuming trading, also known as aggressive trading. The trader uses market orders to fill limit orders already present in the LOB and hence the occurrence of market impact. The area of literature we extend in this paper is focused on liquidity providing trading, also known as passive trading. In this setting the trader is placing limit orders rather than filling them. He must thus wait for a liquidity consuming trader to fill his limit order. Thus a new risk is born, that of non-execution; execution is now a random process. The further into the LOB an order is placed, the higher the payoff for the trader but with a lower probability of execution. As the trader is liquidity providing, the trade off between market impact and price risk is not central to the model. It is instead the trade off between non-execution risk (the aim being to liquidate before some terminal time) and price risk.

This type of model was first suggested by Ho and Stoll (1981) but lay dormant in the literature for some time until Avellaneda and Stoikov (2008) revisited the problem some time later. Under utility maximisation, Avellaneda and Stoikov formulated the problem by considering the statistical properties of the LOB rather than the dynamics itself (see Cont et al., 2010; Cont and De Larrard, 2013). Guéant et al. (2012a) obtained a solution for the problem formulated by Avellaneda and Stoikov. Guéant and Lehalle (2013) extended the problem for general intensity functions, still under a risk-averse utility function, while Bayraktar and Ludkovski (2012) examined the problem for general intensity functions for a risk-neutral trader. Guéant et al. (2012b) examined a single-sided LOB in which a penalty was implemented at the terminal time for assets not sold. Through the use of asymptotic analysis they were able to find solutions in various limits. Under a high-frequency trading framework, Cartea and Jaimungal (2013) proposed a similar model, but including a running penalty for inventory deviations from zero, which complied with the empirical findings of Brunetti et al. (2011).

In this paper we examine two extensions to the liquidity providing trading problem, the first being the liquidation of a correlated portfolio of assets, the second being the liquidation of assets under a stochastic volatility framework. Both of these extensions have been examined for liquidity consuming trading, the former by Schied et al. (2010) and the latter by Almgren (2012), but both have yet to be examined extensively for a liquidity providing trader (Guéant and Lehalle, 2013, derived the HJB PDE for the multi-asset case under standard Brownian motion but did not discuss solutions, either numerically or asymptotically). Correlated assets have been examined in various other areas of finance such as option pricing (see Wilmott, 1998) and portfolio analysis (see Markowitz, 1959), and it is thus natural to extend the optimal liquidation literature in the same manner. Indeed our results can be compared to those of MPT. Many algorithmic trading strategies prefer to have minimal risk on their books (Cartea and Jaimungal, 2013, penalised inventory deviations from zero). When modelling correlated assets the risk in portfolios can sometimes be diversified and thus this analysis becomes of benefit.

Stochastic volatility plays an important role in various areas of financial mathematics and it is the Heston (1993) model that we examine in this paper. Volatility is a key source of uncertainty in the liquidation framework and, given we are examining a risk-averse trader,

makes an important contribution to the solution topology (see Blair et al., 2015). It is thus natural to take into account the non-constant volatility that is observable empirically. Under the Heston framework we introduce a random volatility, correlated with the asset price. It is generally accepted that asset prices and volatility have a negative correlation. As asset prices fall a company becomes riskier, and hence more volatile, as the relative value of debt to equity rises. This is known as the leverage effect (see Black, 1976; Christie, 1987). However, research has also shown that declines in stock prices are accompanied by larger increases in volatility than the decline in volatility that accompanies rising stock markets (see Nelson, 1991; Engle and Ng, 1993).

In our previous paper (see Blair et al., 2015) we extended the literature by examining the liquidation problem of a passive trader under more general diffusion processes for the asset price (which was previously limited to standard Brownian motion), performing a thorough asymptotic analysis of the problem to obtain analytic solutions in various limits. In this paper we shall implement the two extensions under a similar framework. We begin in section 2 by introducing the model for a portfolio of correlated assets, first for the general N asset case before focusing on $N = 2$. We perform a non-dimensionalisation and, with the help of an ansatz solution, reduce the number of variables. We can then formulate the HJB PDE as a classical non-linear PDE by finding the optimal strategy in terms of the value function. We discuss some numerical solutions before doing a thorough asymptotic analysis of the perpetual (steady-state) problem (section 3), as well as various other limits such as small-time-to-termination, which could be beneficial to high-frequency traders. In section 4 we focus on a single asset under a stochastic volatility model, performing a similar dual approach of accurate numerics and asymptotic analysis. We conclude in section 5.

2 Optimal liquidation with multiple underlyings

We consider a trader who wishes to maximise his expected terminal time utility, given a portfolio of assets to liquidate, before a specified terminal time, T. We assume at time $t = 0$ the trader starts with an initial inventory of $q_i(0)$ assets of asset i, in which q_i takes non-negative integer values implying we cannot short sell, and an initial cash holding $X(0)$. Let $(\Omega, \mathcal{F}, \mathbb{P})$ be a probability space with a filtration, $(\mathcal{F}_t, t \in [0, T])$. We assume the reference price[1] $S_i(t)$ of asset i follows a GBM, and so the diffusion process is defined as

$$dS_i(t) = \mu_i S_i(t)dt + \sigma_i S_i(t)dW_i(t), \tag{1}$$

with μ_i as the relative drift, σ_i as the relative volatility and $W_i(t)$ as a Wiener process which is $\mathcal{F}_t$ measurable, with

$$\mathbb{E}[W_i(t)\, W_j(t)] = \rho_{ij} t, \tag{2}$$

in which $\rho_{ij} = \rho_{ji}$, $-1 \leq \rho_{ij} \leq 1$ and $\rho_{ii} = 1$, implying the various assets are correlated for $\rho_{ij} \neq 0$.

The trader will continuously post orders into the ask side of the LOB. For asset i he will post orders for price $S_i^a(t)$ which is $\delta_i = \delta_i(t, X, q_1, \ldots, q_N, S_1, \ldots, S_N)$ percent greater than the reference price $S_i(t)$, i.e.

$$S_i^a(t) = S_i(t)\,(1 + \delta_i)\,. \tag{3}$$

Here we are using the distinct approach, following Blair et al. (2015), of modelling the control as a percent of the asset price rather than having asking price $S^a(t) = S(t) + \delta$, as used previously by various authors (Guéant et al., 2012b; Cartea and Jaimungal, 2013; Avellaneda and Stoikov, 2008, to name a few). Arguments for using this form are discussed in Blair et al..

[1] We use 'reference price' here as given the LOB structure the price at which assets are sold and bought is not the same, as there are various bid and ask prices, with the best bid and ask differing by the spread. As example, the reference price may refer to the best ask or mid-price.

Asset sales follow a time-dependent Poisson process, $N_i(t)$, for asset i, which is $\mathcal{F}_t$ measurable and independent of $W_j(t)$, for all j. The inventory process for asset i is thus

$$dq_i(t) = -dN_i(t). \tag{4}$$

The Poisson processes are uncorrelated and the probability of more than one jump occurring in any infinitisamial small instant Δt is $O\left(\Delta t^2\right)$ and thus negligible to leading order.

For each occurrence of a jump (sale), the trader's cash increases by the amount that asset was sold for, i.e. $S_i(t)\,(1+\delta_i)$. The dynamics of the cash is given by

$$dX(t) = \sum_{i=1}^{N} S_i(t)\,(1+\delta_i)\,dN_i(t), \tag{5}$$

where $N_i(t)$ is the same Poisson process as before. Therefore, when a jump occurs, the values of $q_i(t)$ and $X(t)$ change simultaneously, according to (4) and (5) respectively. We are thus assuming sales are of unitary size, consistent with that of previous literature. $N_i(t)$ has intensity $\Lambda_i(\delta_i)$ which takes the form:

$$\Lambda_i(\delta_i) = \lambda_i \exp\left(-l_i\left(\frac{S_i^a - S_i}{S_i}\right)\right) = \lambda_i e^{-l_i\delta_i}, \tag{6}$$

for some positive constants λ_i and l_i. The liquidity of the market for asset i is described by the intensity of the Poisson process. If no additional amount is added to the reference price then the rate at which the assets are sold is $\Lambda_i(0)$, which for the case of (6) is equal to λ_i. Given the negative exponential form of (6) there is less liquidity for assets sold for prices higher than their reference price and as such the probability of execution is lower. The parameter l_i can be interpreted as the exponential decay factor for the fill rate of orders placed away from the reference price (see Cartea and Jaimungal, 2013), i.e. how quickly or slowly the demand changes as we move further into the LOB and thus how quickly or slowly the probability of execution decreases, which is proportional to the price of the asset. This is different than the standard, absolute decay used in previous literature. Justification for using the form of (6) for the intensity of the Poisson processes is described thoroughly in Avellaneda and Stoikov (2008) which is supported by empirical evidence by Gopikrishnan et al. (2000) and Maslov and Mills (2001) for the distribution of the size of the market orders and by Gabaix et al. (2006), Weber and Rosenow (2005) and Potters and Bouchaud (2003) for the change in price following a market order.

The objective is to liquidate this portfolio before some final time T while maximising the trader's utility. The utility, $\Phi(\cdot)$, we seek to maximise, takes the form of a negative exponential function and as such the trader has CARA defined by

$$A(W) = -\frac{\Phi_{WW}(W)}{\Phi_W(W)}, \tag{7}$$

which for the case of the exponential utility family is constant and equal to the risk aversion parameter, γ, noting the subscript in (7) represents the derivative and W represents the trader's wealth. This form of the utility function is consistent with the previous literature of Avellaneda and Stoikov (2008) and Guéant et al. (2012a,b). We define our value function, $u(t, X, q_1, \ldots, q_N, S_1, \ldots, S_N)$, as the maximum expected utility at time t

$$u(t, X, q_1, \ldots, q_N, S_1, \ldots, S_N) = \sup_{\underline{\delta}(t)\in\mathcal{A}} \mathbb{E}\left[-e^{-\gamma\left(X(T)+\sum_{i=1}^{N} q_i(T)S_i(T)\right)}\right], \tag{8}$$

where $\underline{\delta} = [\delta_1, \ldots, \delta_N]^\top$, $\gamma > 0$ is the risk-aversion characterising the investor and $\mathcal{A} \in (-1, \infty)$ is the set of admissible trading strategies. Assuming the trader starts with some non-negative

wealth and with some positive quantity of inventory the term $\gamma\left(X(T)+\sum_{i=1}^{N} q_i(T)S_i(T)\right)$ is strictly positive. Therefore the objective function, and by definition the value function, are bounded, with $u \in (-1, 0)$. We should note that the lower bound of the admissible strategy occurs naturally due to the investor never wanting to sell his asset for a negative price, implying he would be paying someone to take the asset from him, and hence it does not have to be explicitly implemented.

Given the optimisation problem of (8), an HJB PDE can be derived by applying the Bellman (1957) principle of optimality and using Itō's lemma:

$$\begin{aligned} &u_t + \sum_{i=1}^{N} \mu_i S_i u_{S_i} + \sum_{i=1}^{N}\sum_{j=1}^{N} \frac{1}{2}\rho_{ij}\sigma_i\sigma_j S_i S_j u_{S_i S_j} \\ &+ \sum_{\substack{i=1 \\ q_i>0}}^{N} \sup_{\delta_i} \left[\lambda_i e^{-l_i\delta}\left(u(t, X + S_i\left(1+\delta_i\right), q_1 \ldots, q_i - 1, \ldots, q_N, S_1, \ldots, S_N) - u\right)\right] = 0, \end{aligned} \tag{9}$$

with conditions:[2]

$$u(T, X, q_1, \ldots, q_N, S_1, \ldots, S_N) = \Phi(X, q_1, \ldots, q_N, S_1, \ldots, S_N) = -e^{-\gamma\left(X(T)+\sum_{i=1}^{N} q_i(T)S_i(T)\right)}, \tag{10}$$

and

$$u(t, X, q_i = 0, S_1, \ldots, S_N) = \Phi(X, q_i = 0, S_1, \ldots, S_N) = -e^{-\gamma X(T)} \quad \forall\, i. \tag{11}$$

The derivation of (9) is similar to the derivation of the single asset case which is outlined in Blair et al. (2015), in which a verification theorem is shown. The above problem has dimension $2N + 1$. The focus of this paper will be the $N = 2$ case.

2.1 Problem formulation for two underlyings: reduction and rescaling

For $N = 2$, let $u = u\left(t, X, q_1, q_2, S_1, S_2\right)$. The HJB PDE given by (9) is reduced to

$$\begin{aligned} &u_t + \mu_1 S_1 u_{S_1} + \frac{1}{2}\sigma_1^2 S_1^2 u_{S_1S_1} + \mu_2 S_2 u_{S_2} + \frac{1}{2}\sigma_2^2 S_2^2 u_{S_2S_2} + \rho\sigma_1\sigma_2 S_1 S_2 u_{S_1S_2} \\ &+ \sup_{\delta_1}\left[\lambda_1 e^{-l_1\delta_1}\left(u\left(t, X + S_1\left(1+\delta_1\right), q_1 - 1, q_2, S_1, S_2\right) - u\left(t, X, q_1, q_2, S_1, S_2\right)\right)\right] \\ &+ \sup_{\delta_2}\left[\lambda_2 e^{-l_2\delta_2}\left(u\left(t, X + S_2\left(1+\delta_2\right), q_1, q_2 - 1, S_1, S_2\right) - u\left(t, X, q_1, q_2, S_1, S_2\right)\right)\right] = 0, \end{aligned} \tag{12}$$

with

$$u\left(t = T, q_1, q_2, S_1, S_2\right) = -e^{-\gamma(X+q_1S_1+q_2S_2)}, \tag{13}$$

and

$$u\left(t, q_1 = 0, q_2 = 0, S_2, S_2\right) = -e^{-\gamma X}. \tag{14}$$

If $q_i = 0$ and $q_j > 0$ (12) reduces to

$$\begin{aligned} &u_t + \mu_j S_j u_{S_j} + \frac{1}{2}\sigma_j^2 S_j^2 u_{S_jS_j} \\ &+ \sup_{\delta_j}\left[\lambda_2 e^{-l_j\delta_j}\left(u\left(t, X + S_j\left(1+\delta_j\right), q_i, q_j - 1, S_1, S_2\right) - u\left(t, X, q_i, q_j, S_1, S_2\right)\right)\right] = 0, \end{aligned} \tag{15}$$

[2]In some of the literature, such as Guéant et al. (2012b), a terminal penalty is included such that the assets are sold at a discount of there actual price at the terminal price, while others, such as Avellaneda and Stoikov (2008), Bayraktar and Ludkovski (2012) and Guéant et al. (2012a), neglect inclusion of this terminal penalty. Inclusion of the penalty is quite trivial but in terms of both solving this problem numerically and investigating it asymptotically the terminal penalty would make little difference to both the difficulty of the methods used and the results obtained. We have therefore chosen to neglect it.

as we cannot short sell and thus the derivative terms with respect to S_i are zero as S_i as no impact on the solution.

We can now make a similar reduction as was preformed for the single asset case (15) in Blair et al. (2015)[3]. We introduce the anstaz

$$u(t, X, q_1, q_2, S_1, S_2) = e^{-\gamma X} f(t, q_1, q_2, S_1, S_2), \tag{16}$$

which factors out the cash of the trader, and we then use the following change of variables

$$\tilde{\tau} = \lambda_1 (T - t), \quad \tilde{S}_i = \gamma S_i, \quad \tilde{\mu}_i = \frac{\mu_i}{\lambda_1}, \quad \tilde{\sigma}_i = \frac{\sigma_i}{\sqrt{\lambda_1}}, \quad \tilde{\lambda} = \frac{\lambda_2}{\lambda_1}, \tag{17}$$

noting that $\tilde{S}$ is now the risk-adjusted asset price, given that it is S scaled on γ. From now we will refer to $\tilde{S}$ as the asset price, dropping 'risk-adjusted'. Substituting (16) and (17) into (12) we can solve for the optimal controls δ_i^* by differentiating the supremum with respect to the optimal controls and setting the result equal to zero which locates the stationary point. Solving this we obtain

$$\delta_i^* \left(\tilde{\tau}, q_1, q_2, \tilde{S}_1, \tilde{S}_2\right) = \frac{1}{\tilde{S}_i} \ln \left(\frac{\left(\tilde{S}_i + l_i\right) f\left(\tilde{\tau}, q_i - 1, q_j, \tilde{S}_1, \tilde{S}_2\right)}{l_i f\left(\tilde{\tau}, q_i, q_j, \tilde{S}_1, \tilde{S}_2\right)} \right) - 1, \tag{18}$$

which we notice is independent of X, hence confirming the use of our ansatz solution. Substituting (18), and using (16) and (17), we can transform (12) to

$$\begin{aligned} &- f_{\tilde{\tau}} + \tilde{\mu}_1 \tilde{S}_1 f_{\tilde{S}_1} + \tilde{\mu}_2 \tilde{S}_2 f_{\tilde{S}_2} + \frac{1}{2}\tilde{\sigma}_1^2 \tilde{S}_1^2 f_{\tilde{S}_1\tilde{S}_1} + \frac{1}{2}\tilde{\sigma}_2^2 \tilde{S}_2^2 f_{\tilde{S}_2\tilde{S}_2} + \rho\tilde{\sigma}_1\tilde{\sigma}_2\tilde{S}_1\tilde{S}_2 f_{\tilde{S}_1\tilde{S}_2} \\ &- \frac{e^{l_1}\tilde{S}_1 f}{\tilde{S}_1 + l_1} \left(\frac{l_1 f\left(\tilde{\tau}, q_1, q_2, \tilde{S}_1, \tilde{S}_2\right)}{\left(\tilde{S}_1 + l_1\right) f\left(\tilde{\tau}, q_1 - 1, q_2, \tilde{S}_1, \tilde{S}_2\right)} \right)^{\frac{l_1}{\tilde{S}_1}} \\ &- \frac{\tilde{\lambda} e^{l_2}\tilde{S}_2 f}{\tilde{S}_2 + l_2} \left(\frac{l_2 f\left(\tilde{\tau}, q_1, q_2, \tilde{S}_1, \tilde{S}_2\right)}{\left(\tilde{S}_2 + l_2\right) f\left(\tilde{\tau}, q_1, q_2 - 1, \tilde{S}_1, \tilde{S}_2\right)} \right)^{\frac{l_2}{\tilde{S}_2}} = 0, \end{aligned} \tag{19}$$

with

$$f\left(\tilde{\tau} = 0, q_1, q_2, \tilde{S}_1, \tilde{S}_2\right) = -e^{-q_1\tilde{S}_1 - q_2\tilde{S}_2}, \tag{20}$$

and

$$f\left(\tilde{\tau}, q_1 = 0, q_2 = 0, \tilde{S}_1, \tilde{S}_2\right) = -1. \tag{21}$$

For $q_i = 0$ and $q_j > 0$ (15) can similarly be transformed to

$$-f_{\tilde{\tau}} + \tilde{\mu}_j \tilde{S}_j f_{\tilde{S}_j} + \frac{1}{2}\tilde{\sigma}_j^2 \tilde{S}_j^2 f_{\tilde{S}_j\tilde{S}_j} - \frac{\lambda e^{l_j}\tilde{S}_j f}{\tilde{S}_j + l_j} \left(\frac{l_j f\left(\tilde{\tau}, q_1, q_2, \tilde{S}_1, \tilde{S}_2\right)}{\left(\tilde{S}_j + l_j\right) f\left(\tilde{\tau}, q_i, q_j - 1, \tilde{S}_1, \tilde{S}_2\right)} \right)^{\frac{l_j}{\tilde{S}_j}} = 0, \tag{22}$$

with $\lambda = 1$ if $j = 1$ or $\lambda = \tilde{\lambda}$ if $j = 2$. We note here not only have we reduced the number of input parameters by two but also factored out one of the variables. When discussing results we shall now refer to $f\left(\tilde{\tau}, q_1, q_2, \tilde{S}_1, \tilde{S}_2\right)$ as the value function.

[3]Note this can also be performed for the general N assets case

2.1.1 Boundary conditions

To solve (19) we need boundary conditions in the asset prices, $\tilde{S}_1$ and $\tilde{S}_2$, which must be imposed along lines (rather than points given the extra dimension).

For $\tilde{S}_1 = \tilde{S}_2 = 0$ (19) reduces to

$$\frac{\partial f}{\partial \tilde{\tau}}\left(\tilde{\tau}, q_1, q_2, \tilde{S}_1, \tilde{S}_2\right) = 0. \tag{23}$$

Using this, and (20), we have

$$f\left(\tilde{\tau}, q_1, q_2, \tilde{S}_1 = 0, \tilde{S}_2 = 0\right) = -1. \tag{24}$$

Next we look at the case of $\tilde{S}_i = 0$ while $\tilde{S}_j \neq 0$, for which (19) reduces to the 1-D case in $\tilde{S}_j$ given by (22). Boundary conditions and numerical methods for (22) were discussed in Blair et al. (2015).

Equation (22) has the $\tilde{S}_j = 0$ boundary condition given by (24). For large $\tilde{S}_j$ we use a Neumann boundary condition of the form

$$\frac{\partial f}{\partial \tilde{S}_j}\left(\tilde{\tau}, q_1, q_2, \tilde{S}_1, \tilde{S}_2\right) = 0 \quad \text{as} \quad \tilde{S}_j \to \infty, \tag{25}$$

which is used for both (19), for all values of $\tilde{S}_i$, and (22).

2.1.2 Numerical method

To solve the system (19) we use a finite difference scheme using implicit differences for the derivatives in $\tilde{S}_1$ and $\tilde{S}_2$ and explicit differencing for the non-linear terms. This results in a linear system $\mathbf{Af} = \mathbf{b}$ for each combination of variables q_1, q_2 as well as each time-step, in which all the non-linear terms are on the right-hand-side, i.e. in $\mathbf{b}$. The matrix $\mathbf{A}$ is an $(n \times m) \times (n \times m)$ sparse-banded matrix which consists of $m+1$ subdiagonals and $m+1$ superdiagionals, where n and m are the number of grid points in $\tilde{S}_1$ and $\tilde{S}_2$ respectively. It consists of a main diagonal of parameters, a main superdiagonal of parameters, a main subdiagonal of parameters, $m-3$ superdiagonals of zeros followed by three rows of parameters and $m-3$ subdiagonals of zeros followed by three rows of parameters. The matrix $\mathbf{A}$ is $\tilde{\tau}$ and q_1, q_2 independent. We exploit this by using LU decomposition, in which the matrices $\mathbf{L}$ and $\mathbf{U}$ only need to be calculated once, and, having been stored, can be used repeatedly for all $\tilde{\tau}$ and q_i. We further exploit the sparseness of the matrix by using a NAG (see NAG, 2014) routine *nag_dgbtrf* which takes $O\left((n \times m)^2\right)$ floating point operations which is an order of magnitude smaller than standard Gauss-Elimination to solve the full LU system which takes $O\left((n \times m)^3\right)$ floating point iterations. The NAG routine is also storage efficient as it neglects the zero subdiagonals below the $m^{th}+1$ subdiagonal, as these remain zero after LU decomposition. After using *nag_dgbtrf* to calculate $\mathbf{A} = \mathbf{PLU}$, the NAG routine *nag_dgbtrs* is then used to solve the system $\mathbf{Af} = \mathbf{b}$ which solves $\mathbf{PLY} = \mathbf{B}$ and then $\mathbf{Uf} = \mathbf{Y}$. We expect this routine to be $O\left(\Delta\tilde{\tau}, \Delta\tilde{S}_1^2, \Delta\tilde{S}_2^2\right)$ convergent which was found to be the case. We confirmed our numerics by solving this problem using the Alternating Direction Implicit (ADI) method (see Wilmott, 2007), the successive-over-relaxation (SOR) method (see Cryer, 1971) and a Crank Nicolson finite difference scheme (see Smith, 1965) which results in the need to use an iterative method given the non-linear term, although exhibits $O\left(\Delta\tilde{\tau}^2, \Delta\tilde{S}_1^2, \Delta\tilde{S}_2^2\right)$ convergence. However, implicit differences with explicit non-linear terms was the scheme we used primarily.

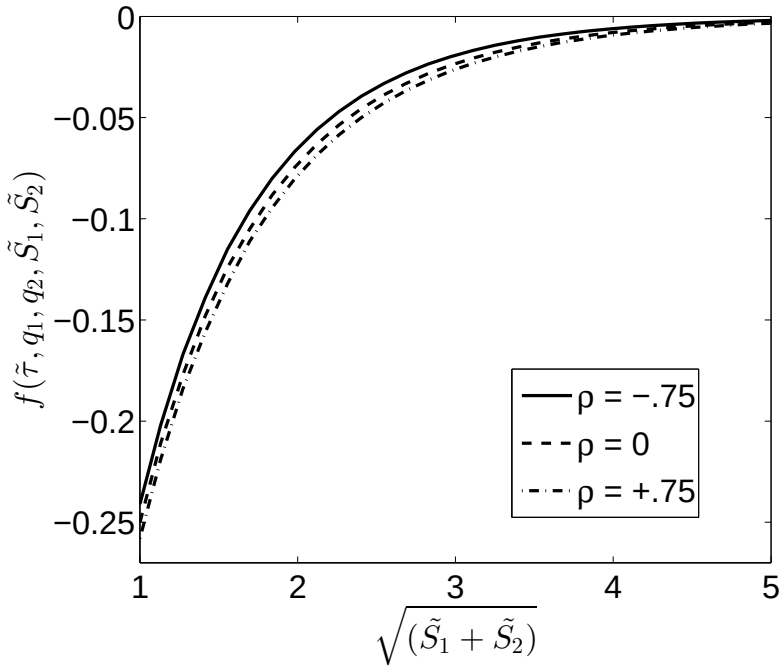

Figure 1: This is a plot of the value function for various values of the correlation parameter ρ, to which we can see the value function is a decreasing function for increasing ρ. The parameters are $\tilde{\mu}_1 = \tilde{\mu}_2 = 0.03, \tilde{\sigma}_1 = \tilde{\sigma}_2 = 0.6, l_1 = l_2 = 10, \tilde{\lambda} = 1$ and varying ρ.

2.1.3 Numerical solutions and discussions

From MPT (see Markowitz, 1959) we expect a trader with negatively correlated assets to want a balance of assets in his portfolio, such that $q_1 = q_2$, while for positively correlated assets the trader would seek an unbalanced portfolio. Figure 1 shows the value function for various values of the correlation parameter, ρ, with otherwise constant parameters, for $q_1 = q_2 = 1$ which is a slice of the main diagonal, corresponding to $\tilde{S}_1 = \tilde{S}_2$. It can be seen how the value is monotonically decreasing as the correlation, ρ, increases, indicating a preference for a negatively correlated portfolio.

We will now shift our attention to the optimal trading strategy for the various regimes of the correlation parameter, ρ. We investigate the optimal trading strategies rather than the value function as these are simply transformations of the value function and, from a financial perspective, are more transparent than examining the value function per se. This can be quite difficult to show graphically given we have $\delta_1^*\left(\tilde{\tau}, q_1, q_2, \tilde{S}_1, \tilde{S}_2\right)$ and $\delta_2^*\left(\tilde{\tau}, q_1, q_2, \tilde{S}_1, \tilde{S}_2\right)$, with q_1 and q_2 taking discrete values. To investigate the optimal trading strategies we will take a slice of the optimal trading strategies δ_1^*, δ_2^* for a single value of time-to-expiry, $\tilde{\tau}$, the price of asset one, $\tilde{S}_1$, and the price of asset two, $\tilde{S}_2$, with $\tilde{\tau} = 1$ and $\tilde{S}_1 = \tilde{S}_2 = 6$. We shall then plot the optimal strategy for asset one, δ_1^*, and the optimal strategy for asset two, δ_2^*, on the vertical axis, with the number of asset two we have remaining, q_2, on the horizontal axis for various values of inventory for asset one, q_1, with $q_1 \geq q_2$ for ease of graphically interpretation. In a corresponding figure, we also plot the optimal strategy of asset one, δ_1^*, and asset two, δ_2^*, on the vertical axis, with the inventory for asset one, q_1, on the horizontal axis, for various values of q_2, with $q_2 \geq q_1$. Although we are plotting discrete points for improved presentation we connect these with lines to show lines of constant q_1 for the former case and q_2 for the latter case, as can be seen in figure 2.

In figure 2(a) the point at which the lines meet corresponds to $q_1 = q_2$. For each point

corresponding to $q_1 = q_2$ we can see that the adjacent line corresponding to the values of the optimal trading strategy for asset one, δ_1^*, increase for increasing inventory of asset two, q_2, while the lines corresponding to the optimal trading strategy of asset two, δ_2^*, decrease for increasing inventory of asset two, q_2. This is due to having more of asset two than asset one as when this is the case the trader seeks to sell asset two faster than asset one so as to balance the risk in his portfolio and hence $\delta_2^* > \delta_1^*$. The same pattern, but with δ_1^* and δ_2^* switched, due to the symmetry, can be seen in figure 2(b). For positively correlated assets, $\rho > 0$, the trading strategies take lower values than that seen in figure 2 as the trader would like to sell quicker to de-risk his portfolio.

We shall now briefly discuss varying parameters such that the symmetry is lost. If the intensity at the best ask, $\tilde{\lambda}$, is increased the values of the optimal strategy of asset one, δ_1^*, decrease while those of asset two, δ_2^*, increase. Increasing $\tilde{\lambda}$ implies the rate at which asset two is sold, assuming all else equal, is a multiple of that of asset one. When the exponential decay of the LOB, l_i, is decreased the optimal trading strategy of asset i, δ_i^*, increases when the asking price is above par value and decreases when the asking price is below par value. When selling above par a lower l_i signifies that the trader can place his asset further into the LOB without significantly reducing his probability of sale. When the trader is eager to sell, he will sell the asset at a discount. In order to do so under lower l_i the trader must sell at a higher discount in order to increase his probability of sale by a significant amount. The opposite is true for larger l_i. If the drift, $\tilde{\mu}_i$, in one asset is increased it will increase the asking price for that asset. This is expected given an asset with a higher expected growth is more valuable than an asset with lower growth. The trader is thus not as keen to sell in comparison to the asset with lower growth as he wants to relinquish the higher growth prospect of the asset while he still holds it. Oppositely, if the volatility, $\tilde{\sigma}_i$, of one asset is increased it will decrease the asking price of that asset. An asset with a higher volatility is more riskier than an asset with lower volatility. The trader thus wants to sell the riskier assets while holding the less risky assets. It is worth noting that altering a parameter for asset i can affect the trading strategy of asset i, δ_i^*, as well as the stratgey of asset j, δ_j^*.

2.2 Small-time-to-termination solution ($\tilde{\tau} \to 0$)

Similar to the single asset case explored in Blair et al. (2015), there is interesting behaviour in the small-time-to-termination regime and thus we examine this next. Using asymptotic analysis we can find a fully analytic solution which is valid in this regime. This could be especially relevant for a high-frequency trading framework given the time remaining would be small and thus analytical expressions would be preferred over numerical solutions.

To examine the small-time-to-termination solution we anticipate a perturbation series about the parameter $\tilde{\tau}$ for $\tilde{\tau} \ll 1$, of the form

$$\begin{aligned} f\left(\tilde{\tau}, q_1, q_2, \tilde{S}_1, \tilde{S}_2\right) &= f_0\left(q_1, q_2, \tilde{S}_1, \tilde{S}_2\right) + \tilde{\tau} f_1\left(q_1, q_2, \tilde{S}_1, \tilde{S}_2\right) \\ &\quad + \tilde{\tau}^2 f_2\left(q_1, q_2, \tilde{S}_1, \tilde{S}_2\right) + O\left(\tilde{\tau}^3\right). \end{aligned} \tag{26}$$

The $O\left(\tilde{\tau}^0\right)$ term, $f_0\left(q_1, q_2, \tilde{S}_1, \tilde{S}_2\right)$, is merely equal to the terminal condition given by (20). By substituting (26) into (19) we can find an analytic solution for $f_1\left(q_1, q_2, \tilde{S}_1, \tilde{S}_2\right)$ by collecting

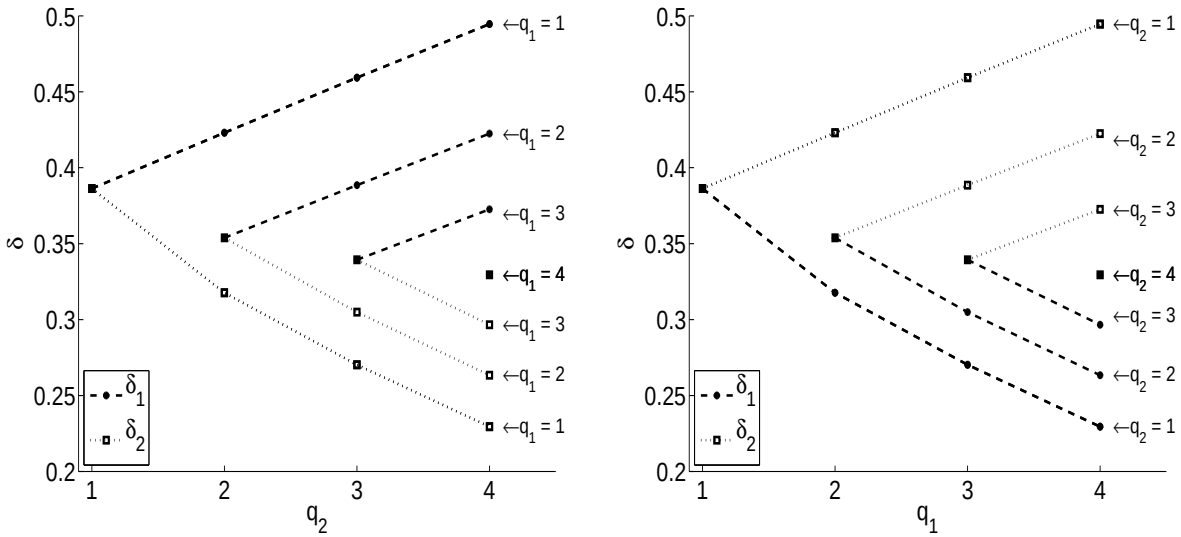

(a) δ_1, δ_2 against q_2

(b) δ_1, δ_2 against q_1

Figure 2: Optimal trading strategy for asset one, δ_1^*, and asset two, δ_2^*, at $\tilde{\tau} = 1, \tilde{S}_1 = \tilde{S}_2 = 6$ for negative correlation ($\rho = -0.75$). The parameters used are $\tilde{\mu}_1 = \tilde{\mu}_2 = 0.03, \tilde{\sigma}_1 = \tilde{\sigma}_2 = 0.1, l_1 = l_2 = 10, \tilde{\lambda} = 1$ and $\rho = -0.75$. It can be seen how the trader has preferences to sell one asset quicker than another in order to achieve a balanced portfolio.

the $O\left(\tilde{\tau}^0\right)$ terms

$$f_1\left(q_1, q_2, \tilde{S}_1, \tilde{S}_2\right) = \Bigg(-\sum_{i=1}^{2} \tilde{\mu}_i \tilde{S}_i q_i + \frac{1}{2}\sum_{i=1}^{2} \tilde{\sigma}_i^2 \tilde{S}_i^2 q_i^2 + \rho\tilde{\sigma}_1\tilde{\sigma}_2\tilde{S}_1\tilde{S}_2 q_1 q_2 \tag{27}$$

$$- \sum_{i=1}^{2} \frac{\tilde{S}_i}{\tilde{S}_i + l_i}\left(\frac{l_i}{\tilde{S}_i + l_i}\right)^{\frac{l_i}{\tilde{S}_i}} \Bigg) f_0\left(q_1, q_2, \tilde{S}_1, \tilde{S}_2\right), \tag{28}$$

and from the $O\left(\tilde{\tau}^1\right)$ terms

$$f_2\left(q_1, q_2, \tilde{S}_1, \tilde{S}_2\right) = \frac{1}{2}\Bigg(\sum_{i-1}^{2} \tilde{\mu}_i \tilde{S}_i f_{1\tilde{S}_i} + \frac{1}{2}\sum_{i=1}^{2} \tilde{\sigma}_i^2 \tilde{S}_i^2 f_{1\tilde{S}_i\tilde{S}_i} + \rho\tilde{\sigma}_1\tilde{\sigma}_2\tilde{S}_1\tilde{S}_2 f_{1\tilde{S}_1\tilde{S}_2}$$

$$-\frac{1}{\tilde{S}_1 + l_1}\left(\frac{l_1}{\tilde{S}_1 + l_1}\right)^{\frac{l_1}{\tilde{S}_1}} \left(\left(l_1 + \tilde{S}_1\right) f_1\left(q_1, q_2, \tilde{S}_1, \tilde{S}_2\right) - l_1 f_1\left(q_1 - 1, q_2, \tilde{S}_1, \tilde{S}_2\right) e^{-\tilde{S}_1}\right)$$

$$-\frac{1}{\tilde{S}_2 + l_2}\left(\frac{l_2}{\tilde{S}_2 + l_2}\right)^{\frac{l_2}{\tilde{S}_2}} \left(\left(l_2 + \tilde{S}_2\right) f_1\left(q_1, q_2, \tilde{S}_1, \tilde{S}_2\right) - l_2 f_1\left(q_1 - 1, q_2, \tilde{S}_1, \tilde{S}_2\right) e^{-\tilde{S}_2}\right)\Bigg), \tag{29}$$

with

$$f_1\left(q_1 = 0, q_2, \tilde{S}_1, \tilde{S}_2\right) = f_1\left(q_1, q_2 = 0, \tilde{S}_1, \tilde{S}_2\right) = 0.$$

In (29) $f_{1\tilde{S}_i}$ and $f_{1\tilde{S}_i\tilde{S}_j}$ are the first and second derivative of f_1, which as we see from (27), can be calculated analytically and as such we have a fully analytic expression for (26). We could include higher-order terms, although this would become increasingly complex.

The approximation (26) is quite accurate even for $\tilde{\tau}$ of $O(1)$ for a range of parameter values, an example of which can be seen in figure 3. This figure shows the full numerical solution compared to the two-term and three-term asymptotic approximation, for both the value function (figure 3(a)) and optimal trading strategy (figure 3(b)). As in the single asset

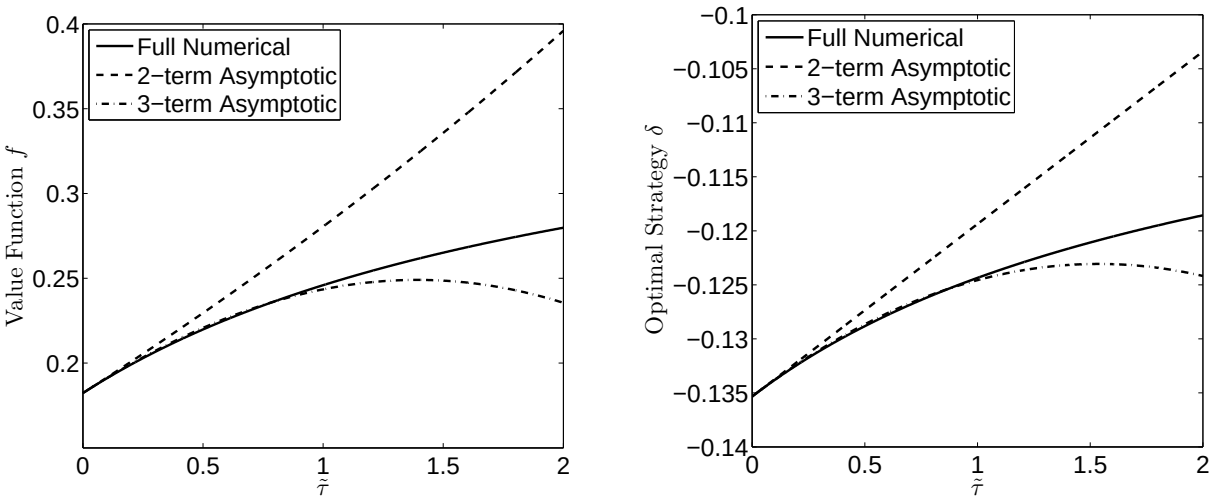

(a) Value function

(b) Optimal Trading Strategy

Figure 3: The two above figures show the small-time approximation (using a first-order and second-order expansion in time) against the solution obtained using the full numerical scheme. This can be seen for both the value function (figure 3(a)) and optimal trading strategy (figure 3(b)). It can be seen that as the number of terms increase the asymptotic solution becomes a better approximation for the full numerical solution. The solutions are functions of time-to-expiry, $\tilde{\tau}$, for $q_1 = q_2 = 1$ at a point along the main diagonal of the solution, so $\tilde{S}_1 = \tilde{S}_2 = 1$. The parameter values used are $\tilde{\mu}_1 = \tilde{\mu}_2 = 0.04, \tilde{\sigma}_1 = \tilde{\sigma}_2 = 0.4, \rho = -0.4, l_1 = l_2 = 5$ and $\lambda = 1$.

case, for which the reader is referred to Blair et al. (2015), there are restrictions to how well the expression holds depending on the parameter values used. For higher values of $\tilde{S}$ and l the solution of $f\left(\tilde{\tau}, q_1, q_2, \tilde{S}_1\tilde{S}_2\right)$ diverges faster from the small-time-to-termination solution due to the stronger presence of the non-linear term.

3 Perpetual problem: multiple underlyings

Numerical simulations positively indicated the possibility that perpetual (time-independent) solutions exist. It is thus of interest to examine these for the multi-dimensional case, by requiring

$$\frac{\partial f}{\partial \tilde{\tau}}\left(\tilde{\tau}, q_1, q_2, \tilde{S}_1, \tilde{S}_2\right) = 0 \quad \text{as} \quad \tilde{\tau} \to \infty.$$

In making this assumption, we are implicitly assuming that the terminal time in which the assets must be sold is sufficiently distant for us to neglect the time variation.

For non-zero q_i the steady-state PDE we examine is

$$\begin{aligned}
&\tilde{\mu}_1\tilde{S}_1 f_{\tilde{S}_1} + \tilde{\mu}_2\tilde{S}_2 f_{\tilde{S}_2} + \frac{1}{2}\tilde{\sigma}_1^2\tilde{S}_1^2 f_{\tilde{S}_1\tilde{S}_1} + \frac{1}{2}\tilde{\sigma}_2^2\tilde{S}_2^2 f_{\tilde{S}_2\tilde{S}_2} + \rho\tilde{\sigma}_1\tilde{\sigma}_2\tilde{S}_1\tilde{S}_2 f_{\tilde{S}_1\tilde{S}_2} \\
&- \frac{e^{l_1}\tilde{S}_1 f}{\tilde{S}_1 + l_1}\left(\frac{l_1 f\left(q_1, q_2, \tilde{S}_1, \tilde{S}_2\right)}{\left(\tilde{S}_1 + l_1\right) f\left(q_1 - 1, q_2, \tilde{S}_1, \tilde{S}_2\right)}\right)^{\frac{l_1}{\tilde{S}_1}} \\
&- \frac{\tilde{\lambda} e^{l_2}\tilde{S}_2 f}{\tilde{S}_2 + l_2}\left(\frac{l_2 f\left(q_1, q_2, \tilde{S}_1, \tilde{S}_2\right)}{\left(\tilde{S}_2 + l_2\right) f\left(q_1, q_2 - 1, \tilde{S}_1, \tilde{S}_2\right)}\right)^{\frac{l_2}{\tilde{S}_2}} = 0,
\end{aligned} \tag{30}$$

with

$$f\left(q_1 = 0, q_2 = 0, \tilde{S}_1, \tilde{S}_2\right) = -1. \tag{31}$$

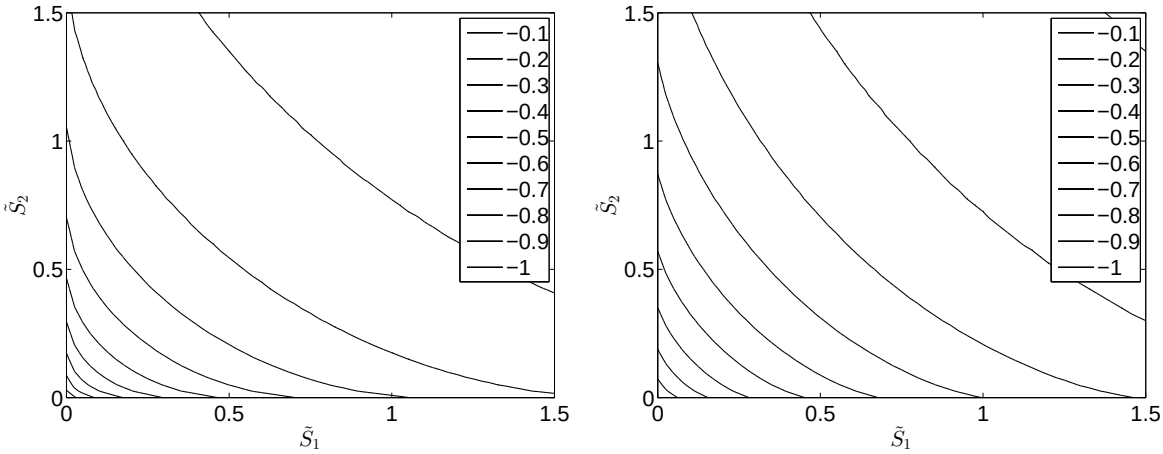

(a) Symmetric case

(b) Asymmetric case

Figure 4: Contours of constant value for the $f\left(q_1 = 1, q_2 = 1, \tilde{S}_1, \tilde{S}_2\right)$ for the symmetric case ($\tilde{\mu}_1 = \tilde{\mu}_2 = 0.04, \tilde{\sigma}_1 = \tilde{\sigma}_2 = 0.4, l_1 = l_2 = 1, \tilde{\lambda} = 1$ and $\rho = -0.4$) and asymmetric case ($\tilde{\mu}_1 = 0.03, \tilde{\mu}_2 = 0.06, \tilde{\sigma}_1 = 0.5, \tilde{\sigma}_2 = 0.7, l_1 = 1, l_2 = 2, \tilde{\lambda} = 2$ and $\rho = -0.4$)

We use the same boundary conditions (22) (with time-derivative equal to zero), (24) and (25) for the perpetual problem as discussed in section 2.1.1 for the non-steady-state problem. When the inventory for asset i is zero, $q_i = 0$, the derivatives with respect to the asset price of asset i, $\tilde{S}_i$, are zero everywhere as $\tilde{S}_i$ has no impact on the solution. As such the problem reduces to the single asset case which was examined thoroughly in Blair et al. (2015).

To solve the steady-state problem we use a Newton-iteration method (see Press et al., 2009). The formulation of this problem results in solving a linear system of equations at each recursive iteration. This allows us to implement the same NAG routine as described in section 2.1.2. However, unlike the non-steady-state case, which has matrix $\mathbf{A}$ that is $\tilde{\tau}$ and q_i independent for all i, the Jacobian matrix used in the Newton iteration (analogous to the matrix $\mathbf{A}$) is a function of $\mathbf{f}$ given the non-linear structure of the PDE and as such is updated at each iteration. Therefore we must perform a LU decomposition at each iteration which can be quite computationally expensive for fine grids. Figure 4(a) shows contours of constant value of the value function. The symmetry in the asset prices of asset one, $\tilde{S}_1$, and asset two, $\tilde{S}_2$, is clear to see, and is on account of the symmetry of the chosen parameters. A second example presented in figure 4(b) shows an analogous contour plot to that of figure 4(a) but with the asset price, $\tilde{S}_1, \tilde{S}_2$, symmetry broken by an asymmetric parameter choice.

It was found in Blair et al. (2015) that there was quite interesting behaviour around the small $\tilde{S}$ region for the perpetual problem. This is also (unsurprisingly) the case for the multi-underlying problem. For zero inventory in asset j, $q_j = 0$, the system is reduced to the single asset case in asset i and thus the same singular behaviour as found in Blair et al. (2015) is present. It is also of interest to examine the case of positive inventory for both assets, $q_1, q_2 > 0$. We shall therefore next examine the small asset price, $\tilde{S}_1, \tilde{S}_2$, solutions.

3.1 Asymptotic analysis of the asset prices $\left(\tilde{S}_1, \tilde{S}_2 \to 0\right)$

Since the PDE (30) appears to have no analytic solutions, we find it useful to use the complimentary approach of asymptotic and numerical methods. Examining figures 4(a) and 4(b) suggests the use of polar coordinates will be advantageous in gaining analytical insight. A similar examination was preformed by Duck et al. (2014) for the case of 2D American options in which converting to polars proved quite insightful and more efficient.

To transform to polar conditions we assign

$$\tilde{S}_1 = R\cos\theta, \qquad \tilde{S}_2 = R\sin\theta, \tag{32}$$

with $R = \left(\tilde{S}_1^2 + \tilde{S}_2^2\right)^{\frac{1}{2}}$. Under this transformation $f\left(q_1, q_2, \tilde{S}_1, \tilde{S}_2\right) = f\left(q_1, q_2, R, \theta\right)$ and as such (30) is transformed to

$$\begin{aligned}
&R^2\left(\frac{1}{2}\tilde{\sigma}_1^2\cos^4\theta + \rho\tilde{\sigma}_1\tilde{\sigma}_2\cos^2\theta\sin^2\theta + \frac{1}{2}\tilde{\sigma}_2^2\sin^4\theta\right) f_{RR} \\
&+ R\cos\theta\sin\theta\left(-\tilde{\sigma}_1^2\cos^2\theta + \rho\tilde{\sigma}_1\tilde{\sigma}_2\left(2\cos^2\theta - 1\right) + \tilde{\sigma}_2^2\sin^2\theta\right) f_{R\theta} \\
&+ \cos^2\theta\sin^2\theta\left(\frac{1}{2}\tilde{\sigma}_1^2 - \rho\tilde{\sigma}_1\tilde{\sigma}_2 + \frac{1}{2}\sigma_2^2\right) f_{\theta\theta} \\
&+ R\left(\cos^2\theta\sin^2\theta\left(\frac{1}{2}\tilde{\sigma}_1^2 - \rho\tilde{\sigma}_1\tilde{\sigma}_2 + \frac{1}{2}\sigma_2^2\right) + \tilde{\mu}_1\cos^2\theta + \tilde{\mu}_2\sin^2\theta\right) f_R \\
&+ \cos\theta\sin\theta\left(\tilde{\sigma}_1^2\cos^2\theta - \rho\tilde{\sigma}_1\tilde{\sigma}_2\left(2\cos^2\theta - 1\right) - \tilde{\sigma}_2^2\sin^2\theta - \tilde{\mu}_1 + \tilde{\mu}_2\right) f_\theta \\
&- \frac{e^{l_1} f R\cos\theta}{R\cos\theta + l_1}\left(\frac{l_1 f\left(q_1, q_2, R, \theta\right)}{\left(R\cos\theta + l_1\right) f\left(q_1 - 1, q_2, R, \theta\right)}\right)^{\frac{l_1}{R\cos\theta}} \\
&- \frac{\tilde{\lambda} e^{l_2} f R\sin\theta}{R\sin\theta + l_2}\left(\frac{l_2 f\left(q_1, q_2, R, \theta\right)}{\left(R\sin\theta + l_2\right) f\left(q_1, q_2 - 1, R, \theta\right)}\right)^{\frac{l_2}{R\sin\theta}} = 0,
\end{aligned} \tag{33}$$

with

$$f\left(q_1 = 0, q_2 = 0, R, \theta\right) = -1. \tag{34}$$

When $\theta = 0$ the PDE reverts to the single asset case in q_1 and $\tilde{S}_1$. Similarly when $\theta = \frac{\pi}{2}$ the PDE reverts to the single asset case in q_2 and $\tilde{S}_2$. We are therefore interested in the behaviour of $\theta \neq \{0, \frac{\pi}{2}\}$, as well as the asymptotic properties as $R \to 0$.

For the single asset case in asset j, i.e. (22) with the time-derivative equal to zero, Blair et al. (2015) found in the limit of the small asset price, $\tilde{S}_j \to 0$, the non-linear term was negligible and the solution behaved like

$$f\left(q, \tilde{S}_j\right) \approx -1 + c(q)\tilde{S}_j^{\beta}, \tag{35}$$

in which

$$\beta = 1 - \frac{2\tilde{\mu}_j}{\tilde{\sigma}_j^2} > 0, \tag{36}$$

with the value of $c\left(q\right)$ found numerically. Asymptotic balancing for the multi-asset case indicates a similar behaviour in the limit as $R \to 0$ and thus (33) is reduced to a linear PDE of the form

$$\begin{aligned}
&R^2\left(\frac{1}{2}\tilde{\sigma}_1^2\cos^4\theta + \rho\tilde{\sigma}_1\tilde{\sigma}_2\cos^2\theta\sin^2\theta + \frac{1}{2}\tilde{\sigma}_2^2\sin^4\theta\right) f_{RR} \\
&+ R\cos\theta\sin\theta\left(-\tilde{\sigma}_1^2\cos^2\theta + \rho\tilde{\sigma}_1\tilde{\sigma}_2\left(2\cos^2\theta - 1\right) + \tilde{\sigma}_2^2\sin^2\theta\right) f_{R\theta} \\
&+ \cos^2\theta\sin^2\theta\left(\frac{1}{2}\tilde{\sigma}_1^2 - \rho\tilde{\sigma}_1\tilde{\sigma}_2 + \frac{1}{2}\sigma_2^2\right) f_{\theta\theta} \\
&+ R\left(\cos^2\theta\sin^2\theta\left(\frac{1}{2}\tilde{\sigma}_1^2 - \rho\tilde{\sigma}_1\tilde{\sigma}_2 + \frac{1}{2}\sigma_2^2\right) + \tilde{\mu}_1\cos^2\theta + \tilde{\mu}_2\sin^2\theta\right) f_R \\
&+ \cos\theta\sin\theta\left(\tilde{\sigma}_1^2\cos^2\theta - \rho\tilde{\sigma}_1\tilde{\sigma}_2\left(2\cos^2\theta - 1\right) - \tilde{\sigma}_2^2\sin^2\theta - \tilde{\mu}_1 + \tilde{\mu}_2\right) f_\theta = 0.
\end{aligned} \tag{37}$$

In the limit as $R \to 0$ it is found that (37) emits two families of solutions, both a homogeneous family and a non-homogeneous family of solution, both of which we will investigate independently.

We shall consider first the non-homogeneous family of solutions, both for the symmetric and asymmetric scenarios. For asymmetric parameters, asymptotic balancing suggests that (37) admits solutions of the form:

$$f = -1 + R^{\hat{\alpha}_1} \hat{f}_1(\theta) + R^{\hat{\alpha}_2} \hat{f}_2(\theta), \tag{38}$$

assuming $\hat{\alpha}_1, \hat{\alpha}_2 > 0$. This results in the linear family of ODEs

$$\begin{aligned}
&\cos^2\theta \sin^2\theta \left(\frac{1}{2}\tilde{\sigma}_1^2 - \rho\tilde{\sigma}_1\tilde{\sigma}_2 + \frac{1}{2}\sigma_2^2\right) \hat{f}_{i\theta\theta} \\
&+ \Bigg(\cos\theta \sin\theta \left(\tilde{\sigma}_1^2 \cos^2\theta - \rho\tilde{\sigma}_1\tilde{\sigma}_2 \left(2\cos^2\theta - 1\right) - \tilde{\sigma}_2^2 \sin^2\theta - \tilde{\mu}_1 + \tilde{\mu}_2\right) \\
&+ \hat{\alpha}_1 \cos\theta \sin\theta \left(-\tilde{\sigma}_1^2 \cos^2\theta + \rho\tilde{\sigma}_1\tilde{\sigma}_2 \left(2\cos^2\theta - 1\right) + \tilde{\sigma}_2^2 \sin^2\theta\right) \Bigg) \hat{f}_{i\theta} \\
&+ \Bigg(\hat{\alpha}_1 \left(\hat{\alpha}_1 - 1\right) \left(\frac{1}{2}\tilde{\sigma}_1^2 \cos^4\theta + \rho\tilde{\sigma}_1\tilde{\sigma}_2 \cos^2\theta \sin^2\theta + \frac{1}{2}\tilde{\sigma}_2^2 \sin^4\theta\right) \\
&+ \hat{\alpha}_1 \left(\cos^2\theta \sin^2\theta \left(\frac{1}{2}\tilde{\sigma}_1^2 - \rho\tilde{\sigma}_1\tilde{\sigma}_2 + \frac{1}{2}\tilde{\sigma}_2^2\right) + \tilde{\mu}_1 \cos^2\theta + \tilde{\mu}_2 \sin^2\theta\right) \Bigg) \hat{f}_i = 0,
\end{aligned} \tag{39}$$

for $i \in \{1, 2\}$.

The next step is to consider the limit of $\hat{f}_1$ and $\hat{f}_2$ as $\theta \to 0$ and $\theta \to \frac{\pi}{2}$. Consider first the solutions of $\hat{f}_1$, examining (39) at $\theta = 0$ we see it reduces to

$$\left(\hat{\alpha}_1 \left(\hat{\alpha}_1 - 1\right) \frac{1}{2}\tilde{\sigma}_1^2 + \hat{\alpha}_1 \tilde{\mu}_1\right) \hat{f}_1 = 0, \tag{40}$$

which for non-zero $\hat{f}_1$ and non-zero $\hat{\alpha}_1$ results in

$$\hat{\alpha}_1 = 1 - \frac{2\tilde{\mu}_1}{\tilde{\sigma}_1^2}, \tag{41}$$

which is analogous with that of the single asset case (see (35),(36)). With $\theta = 0$, which is equivalent to the limit of the small asset price of asset one, $\tilde{S}_1 \to 0$, with $\tilde{S}_2 = 0$, the solution of (38) should match with the single asset case in $\tilde{S}_1$ space and be independent of $\tilde{S}_2$. For this we need that $\hat{f}_1 = c_1(q)$ and $\hat{f}_2 = 0$ at $\theta = 0$, for which $c_i(q)$ represents $c(q)$ in (35).

Turning now to (39) for $i = 2$ we can apply similar analysis. As above, examining (39) at $\theta = \frac{\pi}{2}$ we find

$$\hat{\alpha}_2 = 1 - \frac{2\tilde{\mu}_2}{\tilde{\sigma}_2^2}. \tag{42}$$

Referring to the single asset case, at $\theta = \frac{\pi}{2}$, which is equivalent to the limit of the small asset price of asset two, $\tilde{S}_2 \to 0$, with $\tilde{S}_1 = 0$, the solution of (38) should match with the single asset case in $\tilde{S}_2$ space and be independent of $\tilde{S}_1$. Therefore we need that $\hat{f}_2 = c_2(q)$ and $\hat{f}_1 = 0$ at $\theta = \frac{\pi}{2}$.

We can solve (39) using a central finite difference approach. In (38) it is clearly the least positive of $\hat{\alpha}_1, \hat{\alpha}_2$ that will dominate in the limit as $R \to 0$. The solution f, given by (38), for $q_1 = q_2 = 1$ along the line $\theta = 45°$ can be seen in figure 5(a) along with the solution of (39) which can be seen in figure 5(b).

If we consider the symmetric parameter case, with $\tilde{\sigma}_1 = \tilde{\sigma}_2 = \tilde{\sigma}$ and $\tilde{\mu}_1 = \tilde{\mu}_2 = \tilde{\mu}$, (38) can be reduced to

$$f = -1 + R^{\hat{\alpha}} \hat{f}(\theta), \tag{43}$$

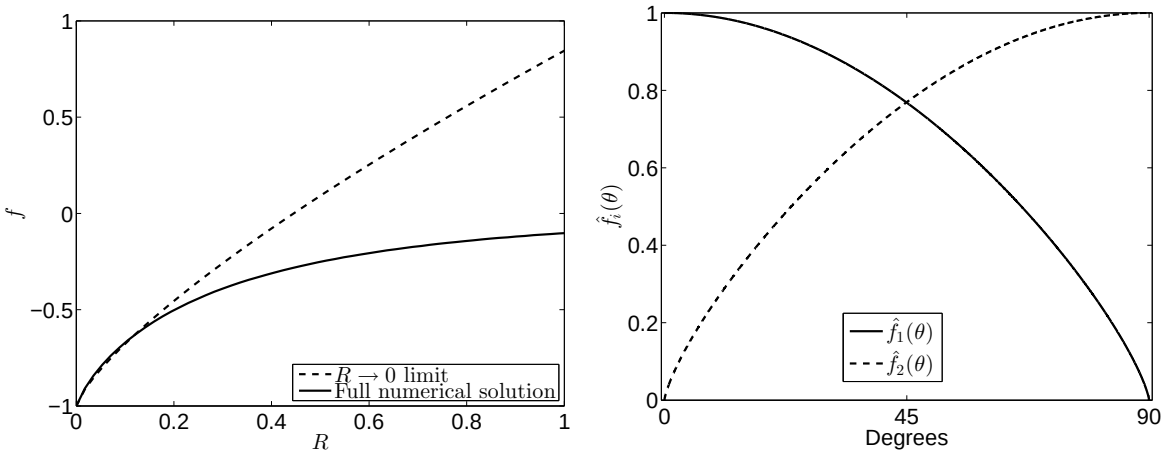

(a) f as $R \to 0$ (b) $\hat{f}(\theta)$

Figure 5: Figure 5(a) shows the solution of f given by (38) as $R \to 0$ alongside the full numerical solution, along the line $\theta = 45°$,with parameter values corresponding to that of figure 4(b). Figure 5(b) shows the solution of $\hat{f}_1(\theta)$ and $\hat{f}_2(\theta)$, which is the solution of the ODEs (39) for $i = 1$ and $i = 2$ respectively, again with parameter values corresponding to that of figure 4(b). Although figure 5(b) looks symmetric we stress it is not.

and rather than a family of ODEs (39) reduces to a single ODE. The value of $\hat{\alpha}$ and the boundary conditions of $\hat{f}(\theta)$ can be deduced in a similar fashion as above. The solution f of (43) for $q_1 = q_2 = 1$ along the line $\theta = 45°$ can be seen in figure 6(a) along with the solution of $\hat{f}(\theta)$ which can be seen in figure 6(b).

Let us now consider the family of solutions which correspond to the homogeneous case, i.e. with boundary conditions:

$$f(\theta = 0) = f(\theta = \pi/2) = 0, \tag{44}$$

for the PDE (37). This PDE emits solutions of the form

$$f = R^{\tilde{\alpha}} \tilde{f}(\theta), \tag{45}$$

which results in the same ODE as (39) with homogeneous boundary conditions of the form

$$\tilde{f}(\theta = 0) = \tilde{f}(\theta = \pi/2) = 0. \tag{46}$$

This implies the problem is a non-linear (quadratic) eigenvalue problem for $\tilde{\alpha}$. In order to address this non-linearity we can introduce a new variable (in the standard way)

$$f^* = \tilde{\alpha}\tilde{f}, \tag{47}$$

and this renders the eigenvalue problem in the system $\left(\tilde{f}, f^*\right)$ a linear one. (39) can thus be

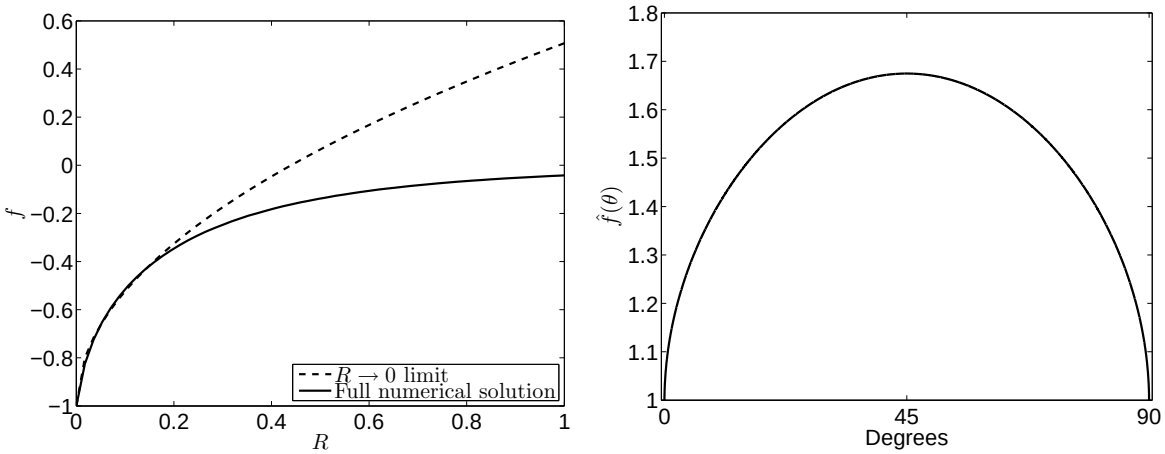

(a) f as $R \to 0$ (b) $\hat{f}(\theta)$

Figure 6: Figure 6(a) shows the solution of f given by (43) as $R \to 0$ alongside the full numerical solution, along the line $\theta = 45°$,with parameter values corresponding to that of figure 4(a). Figure 6(b) shows the solution of $\hat{f}(\theta)$, again with parameter values corresponding to that of figure 4(a).

wrote in the form

$$\begin{aligned}
&\cos^2\theta\sin^2\theta\left(\frac{1}{2}\tilde{\sigma}_1^2 - \rho\tilde{\sigma}_1\tilde{\sigma}_2 + \frac{1}{2}\sigma_2^2\right)\tilde{f}_{\theta\theta} \\
&+ \cos\theta\sin\theta\left(\tilde{\sigma}_1^2\cos^2\theta - \rho\tilde{\sigma}_1\tilde{\sigma}_2\left(2\cos^2\theta - 1\right) - \tilde{\sigma}_2^2\sin^2\theta - \tilde{\mu}_1 + \tilde{\mu}_2\right)\tilde{f}_\theta \\
&+ \left(\left(\cos^2\theta\sin^2\theta\left(\frac{1}{2}\tilde{\sigma}_1^2 - \rho\tilde{\sigma}_1\tilde{\sigma}_2 + \frac{1}{2}\tilde{\sigma}_2^2\right) + \tilde{\mu}_1\cos^2\theta + \tilde{\mu}_2\sin^2\theta\right)\right. \\
&\left. - \left(\frac{1}{2}\tilde{\sigma}_1^2\cos^4\theta + \rho\tilde{\sigma}_1\tilde{\sigma}_2\cos^2\theta\sin^2\theta + \frac{1}{2}\tilde{\sigma}_2^2\sin^4\theta\right)\right)f^* \\
&= -\tilde{\alpha}\cos\theta\sin\theta\left(-\tilde{\sigma}_1^2\cos^2\theta + \rho\tilde{\sigma}_1\tilde{\sigma}_2\left(2\cos^2\theta - 1\right) + \tilde{\sigma}_2^2\sin^2\theta\right)\tilde{f}_\theta \\
&- \tilde{\alpha}\left(\frac{1}{2}\tilde{\sigma}_1^2\cos^4\theta + \rho\tilde{\sigma}_1\tilde{\sigma}_2\cos^2\theta\sin^2\theta + \frac{1}{2}\tilde{\sigma}_2^2\sin^4\theta\right)f^*. \qquad (48)
\end{aligned}$$

Using second-order differencing on (48), with boundary conditions given by (46), coupled with (47) we can write the system as:

$$\mathbf{AX} = \tilde{\alpha}\mathbf{BX}, \qquad (49)$$

with $\tilde{\alpha}$ as the eigenvalues and the corresponding eigenvectors being X, which contains both $\tilde{f}$ and f^*. The numerical set-up is such that if we discretise $\tilde{f}$ into n grid points, the matrices $\mathbf{A}$ and $\mathbf{B}$ will be size $2n \times 2n$, with corresponding elements alternating between the parameter values of $\tilde{f}$ and f^*. Given this problem formulation we can treat the problem as an algebraic generalised eigenvalue problem, using a QZ algorithm.

Computations indicated conclusively that no complex eigenvalue $\tilde{\alpha}$ exist, although both positive and negative values were found. For this problem it is the positive eigenvalues that are of interest for $R \to 0$, particularly the smallest positive eigenvalue as this will exhibit the slowest decay in this region. Figure 7 shows results for the smallest positive value of $\tilde{\alpha}$ for a range of values of the drift of asset one, $\tilde{\mu}_1$, one curve for $\tilde{\mu}_2 = \tilde{\mu}_1$, the other for $\tilde{\mu}_2 = 0.05$. Other parameters are those used previously in figure 4(a), namely volatility $\tilde{\sigma}_1 = \tilde{\sigma}_2 = 0.4$ and correlation $\rho = -0.4$. Numerical results indicate that there are a (likely infinite) discrete set of eigenvalues $\tilde{\alpha}$. A plot of the eigenvector $\tilde{f}(\theta)$ corresponding to the smallest positive $\tilde{\alpha}$ can be seen in figure 8.

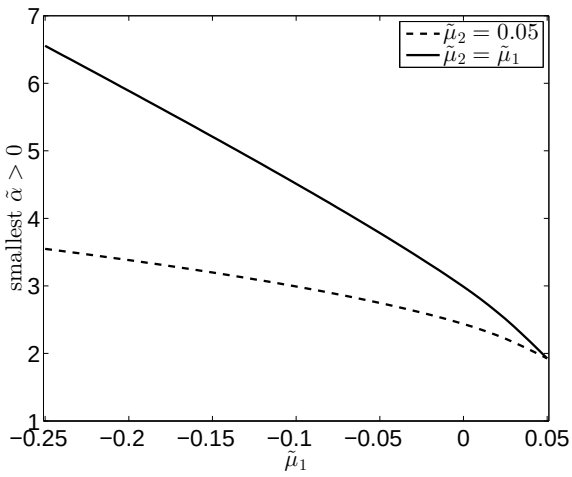

Figure 7: Variation of smallest positive $\tilde{\alpha}$ with $\tilde{\mu}_1$, for the case of $\tilde{\mu}_2 = \tilde{\mu}_1$ and $\tilde{\mu}_2 = 0.05$. The rest of the parameters match that of figure 4(a), that being $\tilde{\sigma}_1 = \tilde{\sigma}_2 = 0.4$ and $\rho = -0.4$.

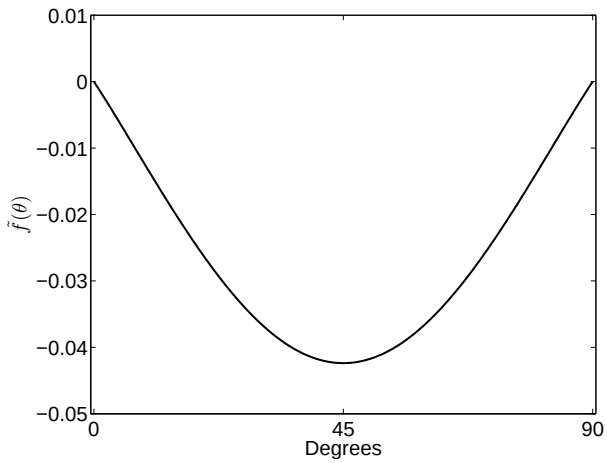

Figure 8: $\tilde{f}(\theta)$ for smallest positive $\tilde{\alpha} = 2.17$. The parameters match that of figure 4(a), that being $\tilde{\mu}_1 = \tilde{\mu}_2 = 0.04, \tilde{\sigma}_1 = \tilde{\sigma}_2 = 0.4$ and $\rho = -0.4$.

Given the non-homogeneous and homogeneous solutions we have discussed we conclude in the limit as $R \to 0$ the solution can be wrote as an infinite series of the form:

$$f = -1 + R^{\hat{\alpha}_1} \hat{f}_1(\theta) + R^{\hat{\alpha}_2} \hat{f}_2(\theta) + \sum_{i=0}^{\infty} R^{\tilde{\alpha}_i} \tilde{f}_i(\theta), \tag{50}$$

with the *hat* terms being solutions of the non-homogeneous problem and the *tilde* terms being the solutions of the homogeneous (eigenvalue) problem. As $R \to 0$ it is the smallest positive value of $\hat{\alpha}_1, \hat{\alpha}_2, \tilde{\alpha}_i$ that will have the corresponding dominant behaviour. For the parameter values used in the example shown in figure 4(a) we have $\hat{\alpha}_1 = \hat{\alpha}_2 = 0.5$ and the smallest positive eigenvalue $\tilde{\alpha}_i$ takes the value $\tilde{\alpha}^+_{\min} = 2.17$. For this example it is thus the non-homogeneous family of solutions which dominate.

3.2 Large inventory solution $(q_1, q_2 \to \infty)$

We can investigate a large inventory solution for the multi-asset case such that q_1 and/or q_2 become large (both together and individually).

Similar to the single asset case, numerical simulations and asymptotic analysis lead us to conclude

$$\lim_{q_i \to \infty} \left(\frac{f\left(q_1, \ldots, q_i, \ldots, q_N, \tilde{S}_1, \ldots, \tilde{S}_N\right)}{f\left(q_1, \ldots, q_i - 1, \ldots, q_N, \tilde{S}_1, \ldots, \tilde{S}_N\right)} \right) \to 1. \tag{51}$$

For the case of only one amount of inventory tending to infinity, say $q_2 \to \infty$ and $q_1 \sim O(1)$ (30) reduces to

$$\begin{aligned} &\tilde{\mu}_1 \tilde{S}_1 f_{\tilde{S}_1} + \tilde{\mu}_2 \tilde{S}_2 f_{\tilde{S}_2} + \frac{1}{2}\tilde{\sigma}_1^2 \tilde{S}_1^2 f_{\tilde{S}_1\tilde{S}_1} + \frac{1}{2}\tilde{\sigma}_2^2 \tilde{S}_2^2 f_{\tilde{S}_2\tilde{S}_2} + \rho\tilde{\sigma}_1\tilde{\sigma}_2 \tilde{S}_1 \tilde{S}_2 f_{\tilde{S}_1\tilde{S}_2} \\ &- \frac{e^{l_1}\tilde{S}_1 f}{\tilde{S}_1 + l_1} \left(\frac{l_1 f\left(q_1, \tilde{S}_1, \tilde{S}_2\right)}{\left(\tilde{S}_1 + l_1\right) f\left(q_1 - 1, \tilde{S}_1, \tilde{S}_2\right)} \right)^{\frac{l_1}{\tilde{S}_1}} - \frac{\tilde{\lambda} e^{l_2} \tilde{S}_2 f}{\tilde{S}_2 + l_2} \left(\frac{l_2}{\left(\tilde{S}_2 + l_2\right)} \right)^{\frac{l_2}{\tilde{S}_2}} = 0, \end{aligned} \tag{52}$$

with $f = f\left(q_1, \tilde{S}_1, \tilde{S}_2\right)$ and boundary conditions analogous to those discussed in section 2.1.1. For $q_2 \to \infty$, we only consider the case of the inventory of asset one being positive, $q_1 > 0$, as $q_1 = 0$ is identical to the single asset case examined in Blair et al. (2015). (52) is still a non-linear PDE and thus an iterative method must be used with appropriate boundary conditions in the asset prices, $\tilde{S}_1$ and $\tilde{S}_2$. To solve (52) we use a similar iterative method as described above for the perpetual case when the inventory was of order one, $q_1, q_2 \sim O(1)$, and use the same boundary conditions in the asset prices, $\tilde{S}_1$ and $\tilde{S}_2$. A solution for (52) can be seen in figure 9, in which figure 9(a) is a surface plot of $f\left(q_1 = 1, q_2 \to \infty, \tilde{S}_1, \tilde{S}_1\right)$, along with a contour plot in figure 9(b). Figure 9(a) shows the rapid decay to zero as the price of asset two, $\tilde{S}_2$, increases, while at $\tilde{S}_2 = 0$ we see the more gentle decay, corresponding to $q_1 = 1$. This is also portrayed in figure 9(b), which we can compare to figure 4(a) which is the case of $q_1 = q_2 = 1$.

We can also examine the case of when both the inventory of asset one and asset two are large, $q_1, q_2 \to \infty$, in which the non-linear PDE (52) reduces to the *linear* PDE:

$$\begin{aligned} &\tilde{\mu}_1 \tilde{S}_1 f_{\tilde{S}_1} + \tilde{\mu}_2 \tilde{S}_2 f_{\tilde{S}_2} + \frac{1}{2}\tilde{\sigma}_1^2 \tilde{S}_1^2 f_{\tilde{S}_1\tilde{S}_1} + \frac{1}{2}\tilde{\sigma}_2^2 \tilde{S}_2^2 f_{\tilde{S}_2\tilde{S}_2} + \rho\tilde{\sigma}_1\tilde{\sigma}_2 \tilde{S}_1 \tilde{S}_2 f_{\tilde{S}_1\tilde{S}_2} \\ &- \frac{e^{l_1}\tilde{S}_1 f}{\tilde{S}_1 + l_1} \left(\frac{l_1}{\left(\tilde{S}_1 + l_1\right)} \right)^{\frac{l_1}{\tilde{S}_1}} - \frac{\tilde{\lambda} e^{l_2} \tilde{S}_2 f}{\tilde{S}_2 + l_2} \left(\frac{l_2}{\left(\tilde{S}_2 + l_2\right)} \right)^{\frac{l_2}{\tilde{S}_2}} = 0, \end{aligned} \tag{53}$$

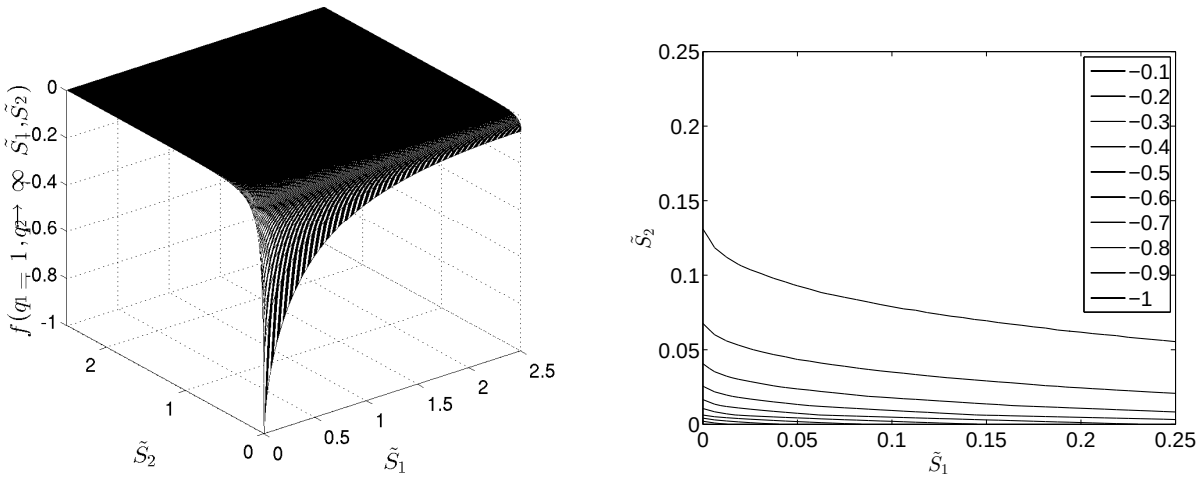

(a) $f\left(q_1 = 1, q_2 \to \infty, \tilde{S}_1, \tilde{S}_1\right)$ mesh plot

(b) $f\left(q_1 = 1, q_2 \to \infty, \tilde{S}_1, \tilde{S}_1\right)$ contour plot

Figure 9: Plot of $q_1 = 1$ with $q_2 \to \infty$ as a surface plot and contour plot with parameter values $\tilde{\mu}_1 = \tilde{\mu}_2 = 0.04, \tilde{\sigma}_1 = \tilde{\sigma}_2 = 0.4, l_1 = l_2 = 1, \tilde{\lambda} = 1$ and $\rho = -0.4$

with $f = f\left(\tilde{S}_1, \tilde{S}_2\right)$ with the same boundary conditions to those above for inventory of order one, $q_1, q_2 \sim O(1)$. As this is a linear PDE we need not use an iterative method (the boundary conditions as used for the non-linear case remain valid). A solution of (53) can be seen in figure 10. In figure 10(a) we show the convergence of increasing q_1, q_2. This figure shows curves along the main diagonal of the asset prices, i.e. $\tilde{S}_1 = \tilde{S}_2$, for $f\left(q_1 = q_2, \tilde{S}_1, \tilde{S}_2\right)$ (solid line), $f\left(q_1 = 1, q_2 \to \infty, \tilde{S}_1, \tilde{S}_2\right)$ (dot-dash line) and $f\left(q_1 \to \infty, q_2 \to \infty, \tilde{S}_1\tilde{S}_2\right)$ (broken line). We see the solution of $f\left(q_1, q_2, \tilde{S}_1\tilde{S}_2\right)$, for $q_1, q_2 \sim O(1)$, converges to $f\left(q_1 = 1, q_2 \to \infty, \tilde{S}_1\tilde{S}_2\right)$ which converges to $f\left(q_1 \to \infty, q_2 \to \infty, \tilde{S}_1\tilde{S}_2\right)$. Figure 10(b) is a contour plot of $f\left(q_1 \to \infty, q_2 \to \infty, \tilde{S}_1\tilde{S}_2\right)$, which is comparable to that of figure 9(b) and figure 4(a).

4 A single underlying with stochastic volatility

We shall now examine when the trader has a quantity $q(0)$ of a single underlying asset to liquidate, but for which the volatility of this underlying is assumed stochastic. We shall consider a similar framework as previous in which a trader wishes to maximise his expected terminal time utility. Let $(\Omega, \mathcal{F}, \mathbb{P})$ be a probability space with a filtration, $(\mathcal{F}_t, t \in [0, T])$. We follow Heston (1993) by assuming the asset follows

$$dS(t) = \mu S(t)\, dt + \sqrt{\nu(t)} S(t)\, dW(t), \tag{54}$$

with the square-root of the variance $\nu(t)$ following the Uhlenbeck and Ornstein (1930) process

$$d\sqrt{\nu(t)} = -\beta\sqrt{\nu(t)}dt + \alpha dB(t). \tag{55}$$

It can be shown through Itō's lemma that the variance $\nu(t)$ follows the process

$$d\nu(t) = \left(\delta^2 - 2\beta\nu(t)\right) dt + 2\alpha\sqrt{\nu(t)}dB(t), \tag{56}$$

which can be represented as a square-root process (Cox et al., 1985)

$$d\nu(t) = \kappa(\theta - \nu(t))\, dt + \sigma\sqrt{\nu(t)}dB(t), \tag{57}$$

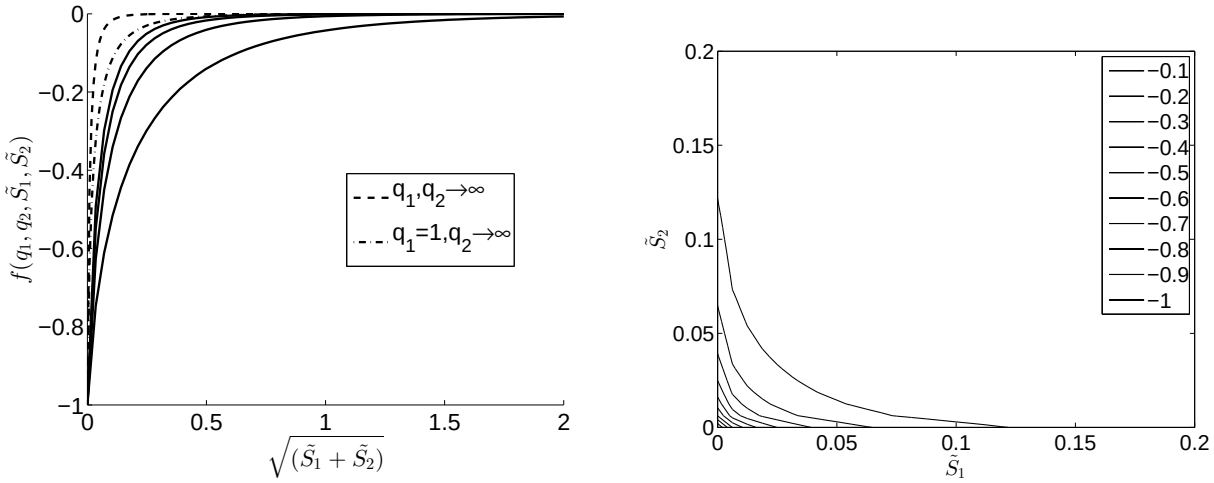

(a) $f\left(q_1, q_2, \tilde{S}_1, \tilde{S}_2\right)$ for various limits

(b) $f\left(q_1 = q_2 \to \infty, \tilde{S}_1, \tilde{S}_1\right)$ contour plot

Figure 10: Figure 10(a) shows curves of the main diagonal of the asset price, i.e. $\tilde{S}_1 = \tilde{S}_2$, for $f\left(q_1 = q_2, \tilde{S}_1, \tilde{S}_2\right)$ (solid line), $f\left(q_1 = 1, q_2 \to \infty, \tilde{S}_1, \tilde{S}_2\right)$ (dot-dash line) and $f\left(q_1 \to \infty, q_2 \to \infty, \tilde{S}_1, \tilde{S}_2\right)$ (broken line) in which we see the $q_1, q_2 \sim O(1)$ solution converges to $f\left(q_1 = 1, q_2 \to \infty, \tilde{S}_1, \tilde{S}_2\right)$ which converges to $f\left(q_1 \to \infty, q_2 \to \infty, \tilde{S}_1, \tilde{S}_2\right)$. Figure 10(b) shows the solution of (53) as a contour plot. The parameter values $\tilde{\mu}_1 = \tilde{\mu}_2 = 0.04, \tilde{\sigma}_1 = \tilde{\sigma}_2 = 0.04, l_1 = l_2 = 1, \tilde{\lambda} = 1$ and $\rho = -0.4$

with $\mathbb{E}[W(t)\,B(t)] = \rho t$, such that the asset price and variance are correlated.

The value function we define, $u(t, X, q, S, \nu)$, is now a function of the variance, ν, and is defined as the maximum expected utility at time t

$$u(t, X, q, S, \nu) = \sup_{\delta(t) \in \mathcal{A}} \mathbb{E}\left[-e^{-\gamma(X(T)+q(T)S(T))}\right]. \tag{58}$$

The inventory and cash follow (4) and (5) respectively for $N = 1$, with the Poisson process being independent of the Brownian motions, and having intensity defined by (6).

We can define the HJB PDE as

$$\begin{aligned} u_t + \mu S u_S + \frac{1}{2}\nu S^2 u_{SS} + \kappa(\theta - \nu) u_\nu + \frac{1}{2}\sigma^2 \nu u_{\nu\nu} + \rho\sigma\nu S u_{S\nu} \\ + \sup_{\delta}\left[\lambda e^{-l\delta}\left(u(t, X + S(1+\delta), q-1, S, \nu) - u(t, X, q, S, \nu)\right)\right] = 0, \end{aligned} \tag{59}$$

with initial conditions

$$u(T, X, q, S, \nu) = -e^{-\gamma(X+qS)}, \tag{60}$$

and

$$u(t, X, 0, S, \nu) = -e^{-\gamma X}. \tag{61}$$

The derivation of this HJB PDE is a relatively straightforward extension to that of the constant volatility case and the reader is referred to Blair et al. (2015) for further details. Extending the verification theorem from the constant volatility case is also straightforward and is thus not detailed here.

As in section 2.1 we introduce an ansatz

$$u(t, X, q, S, \nu) = e^{-\gamma X} f(t, q, S, \nu), \tag{62}$$

and perform a change of variables

$$\tilde{\tau} = \lambda (T - t), \quad \tilde{S} = S\gamma, \quad \tilde{\nu} = \frac{\nu}{\lambda}, \quad \tilde{\theta} = \frac{\theta}{\lambda}, \quad \tilde{\mu} = \frac{\mu}{\lambda}, \tag{63}$$

such that all the *tilde* variables are dimensionless. This results in the non-linear dimensionless PDE

$$\begin{aligned} &- f_{\tilde{\tau}} + \tilde{\mu}\tilde{S} f_{\tilde{S}} + \frac{1}{2}\tilde{\nu}\tilde{S}^2 f_{\tilde{S}\tilde{S}} + \kappa\left(\tilde{\theta} - \tilde{\nu}\right) f_{\tilde{\nu}} + \frac{1}{2}\sigma^2\tilde{\nu} f_{\tilde{\nu}\tilde{\nu}} + \rho\sigma\tilde{\nu}\tilde{S} f_{\tilde{S}\tilde{\nu}} \\ &- \frac{e^l \tilde{S} f}{\tilde{S} + l}\left(\frac{l f\left(\tilde{\tau}, q, \tilde{S}, \tilde{\nu}\right)}{\left(\tilde{S} + l\right) f\left(\tilde{\tau}, q - 1, \tilde{S}, \tilde{\nu}\right)}\right)^{\frac{l}{\tilde{S}}} = 0, \end{aligned} \tag{64}$$

with $f = f\left(\tilde{\tau}, q, \tilde{S}, \tilde{\nu}\right)$ and initial conditions

$$f\left(0, q, \tilde{S}, \tilde{\nu}\right) = -e^{-q\tilde{S}}, \tag{65}$$

and

$$f\left(\tau, 0, \tilde{S}, \tilde{\nu}\right) = -1, \tag{66}$$

in which we have factored out the γ and λ parameter. The optimal trading strategy for the non-dimensional case is given by

$$\delta^*\left(\tilde{\tau}, q, \tilde{S}, \tilde{\nu}\right) = \frac{1}{\tilde{S}} \ln\left(\frac{\left(\tilde{S} + l\right) f\left(\tilde{\tau}, q - 1, \tilde{S}, \tilde{\nu}\right)}{l f\left(\tilde{\tau}, q, \tilde{S}, \tilde{\nu}\right)}\right) - 1. \tag{67}$$

To solve (64) we require two boundary conditions in each of the two semi-infinite domains of the asset price, $\tilde{S}$, and variance, $\tilde{\nu}$. As $\tilde{S} \to 0$, (64) reduces to

$$-f_{\tilde{\tau}} + \kappa\left(\tilde{\theta} - \tilde{\nu}\right) f_{\tilde{\nu}} + \frac{1}{2}\sigma^2\tilde{\nu} f_{\tilde{\nu}\tilde{\nu}} = 0. \tag{68}$$

Similarly, as $\tilde{\nu} \to 0$, (64) reduces to

$$-f_{\tilde{\tau}} + \tilde{\mu}\tilde{S} f_{\tilde{S}} + \kappa\tilde{\theta} f_{\tilde{\nu}} - \frac{e^l \tilde{S} f}{\tilde{S} + l}\left(\frac{l f\left(\tilde{\tau}, q, \tilde{S}, \tilde{\nu}\right)}{\left(\tilde{S} + l\right) f\left(\tilde{\tau}, q - 1, \tilde{S}, \tilde{\nu}\right)}\right)^{\frac{l}{\tilde{S}}} = 0. \tag{69}$$

As both $\tilde{S} \to 0$ and $\tilde{\nu} \to 0$, (68) and (69) reduce to

$$\frac{\partial f}{\partial \tilde{\tau}}\left(\tilde{\tau}, q, \tilde{S} \to 0, \tilde{\nu} \to 0\right) = 0 \quad \Rightarrow \quad f\left(\tilde{\tau}, q, \tilde{S} \to 0, \tilde{\nu} \to 0\right) = -1, \tag{70}$$

which arises from the initial condition (65). Similar to previous cases as $\tilde{S} \to \infty$ we use a Neumann condition of the form

$$\frac{\partial f}{\partial \tilde{S}}\left(\tilde{\tau}, q, \tilde{S} \to \infty, \tilde{\nu}\right) = 0. \tag{71}$$

We use a similar condition for the case of the variance tending to infinity which takes the form

$$\frac{\partial f}{\partial \tilde{\nu}}\left(\tilde{\tau}, q, \tilde{S}, \tilde{\nu} \to \infty\right) = 0. \tag{72}$$

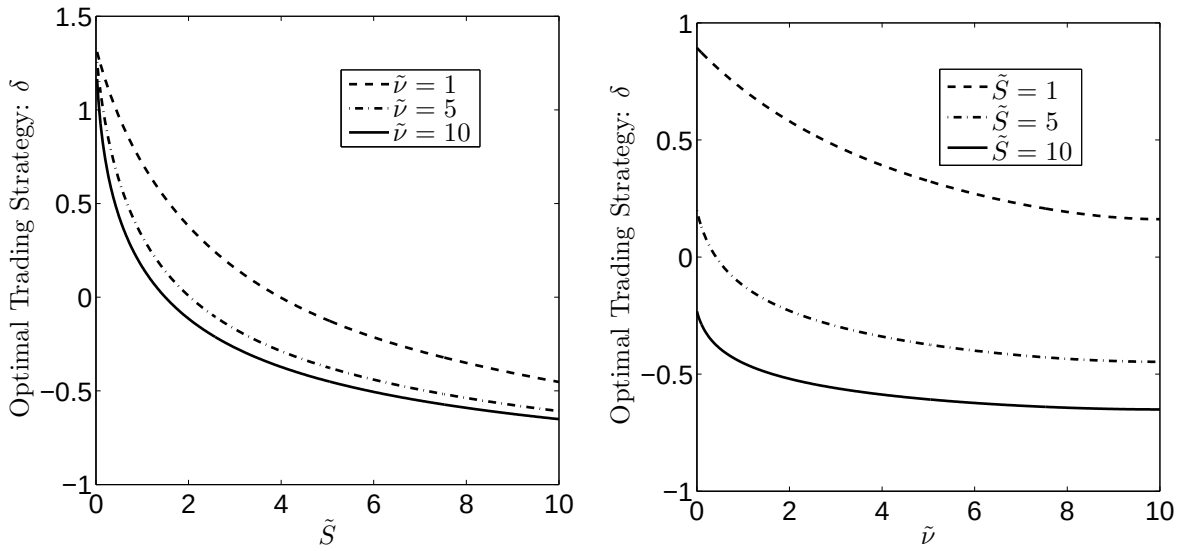

(a) δ against $\tilde{S}$, varying $\tilde{\nu}$

(b) δ against $\tilde{\nu}$, varying $\tilde{S}$

Figure 11: The above figures show the optimal trading strategy, δ^*, plotted against the asset price, $\tilde{S}$, (figure 11(a)) and against the variance, $\tilde{\nu}$, (figure 11(b)). The parameter values used are $\tilde{\tau} = 1, l = 1, \tilde{\mu} = 0.02, \kappa = 0.75, \tilde{\theta} = 0.46, \sigma = 2.78$ and $\rho = -0.64$.

Intuitively, the higher the volatility the lower the trader's value function as he is more risk-averse. Thus the derivative of the value with respect to $\tilde{\nu}$ is decreasing which can be approximated as zero when $\tilde{\nu} \to \infty$.

To solve this problem numerically we use a similar implicit-explicit finite difference scheme to that as used in the multiple-underlying case. The trading strategies can be in found in figure 11(a) and figure 11(b). It can be seen in both figures that the optimal strategy δ^* is decreasing as the asset price, $\tilde{S}$, and variance, $\tilde{\nu}$, increase. As the risk-adjusted asset price increases the trader would like to sell quicker to lock in profit. Similarly, a higher variance represents a riskier portfolio for the trader and given the trader is risk-averse he would have preference over a lower variance.

To gain further insight into how the solutions depend on the various parameters we shall consider the optimal trading strategies while keeping all but one parameter constant. We first investigate altering the speed of reversion, κ. For larger values of κ the speed of reversion to the long-term mean, $\tilde{\theta}$, is faster. It can seen in figure 12 that when $\tilde{\nu} < \tilde{\theta}$ the variance is expected to increase and a such a lower value of κ is preferred so it increases slowly. In contrast, when $\tilde{\nu} > \tilde{\theta}$ the variance is expected to decrease and a such a higher value of κ is preferred so it decreases quickly.

Figures 13(a) and 13(b) each have three curves corresponding to different values of the correlation parameter, $\rho = \{-0.64, 0.00, +0.64\}$. In both we can see there is a switch in preference of whether a positive or negative correlation is preferred. A positive correlation is preferred when the variance, $\tilde{\nu}$, is small and expected to increase back to its long-term mean, while a negative correlation is preferred when $\tilde{\nu}$ is large and expected to decrease back to its long-term mean.

Numerical simulations suggested it is favourable to have a smaller value of the long-term mean of the variance, $\tilde{\theta}$, for all values of the asset price, $\tilde{S}$, and variance, $\tilde{\nu}$, as this indicates the smallest expected long-term level of variance, and as discussed above, smaller variance is preferred over higher variance.

Investigation of the affect of σ, the volatility of variance, proved quite interesting. It was found that in certain regimes a smaller σ was preferred, such as when the variance was below

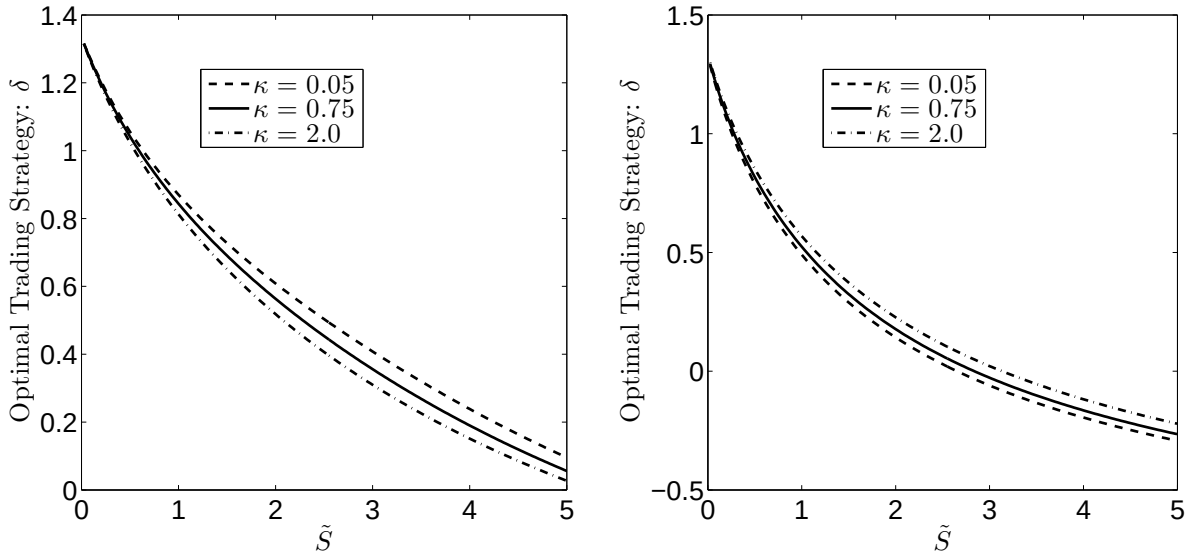

(a) δ against $\tilde{S}$, varying κ with $\tilde{\nu} < \tilde{\theta}$

(b) δ against $\tilde{S}$, varying κ with $\tilde{\nu} > \tilde{\theta}$

Figure 12: The above figures show the optimal trading strategy, δ^*, plotted against the asset price, $\tilde{S}$, for various values of the rate of reversion parameter, κ, with variance $\tilde{\nu} = 0.25 < \tilde{\theta}$ (figure 12(a)) and $\tilde{\nu} = 2.5 > \tilde{\theta}$ (figure 12(b)). The parameter values used are $\tilde{\tau} = 1, l = 1, \tilde{\mu} = 0.02, \kappa = \{0.05, 0.75, 2.0\}, \tilde{\theta} = 0.46, \sigma = 2.78$ and $\rho = -0.64$.

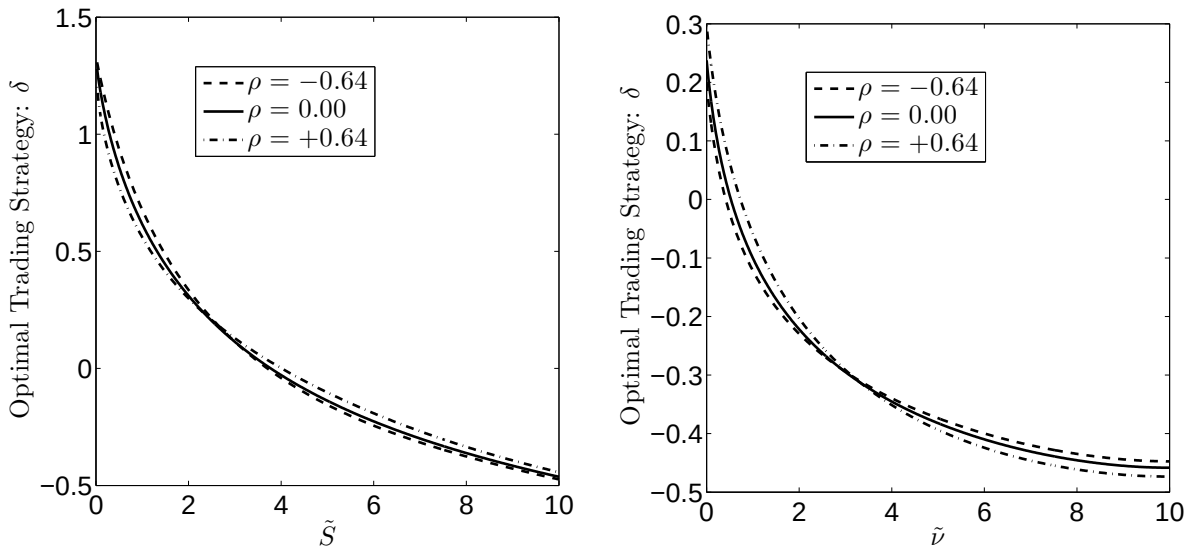

(a) δ against $\tilde{S}$, varying ρ

(b) δ against $\tilde{\nu}$, varying ρ

Figure 13: The above figures show the optimal trading strategy, δ^*, for various values of the correlation parameter ρ plotted against the asset price $\tilde{S}$ (figure 13(a), with $\tilde{\nu} = 1.25$) and against the variance $\tilde{\nu}$ (figure 13(b), with $\tilde{\nu} = 5.00$). The parameter values used are $\tilde{\tau} = 1, l = 1, \tilde{\mu} = 0.02, \kappa = 0.75, \tilde{\theta} = 0.46, \sigma = 2.78$ and $\rho = \{-0.64, 0.0, +0.64\}$.

the long-term mean, $\tilde{\theta}$, as being risk-averse the trader prefers more certainty. However, when the variance, $\tilde{\nu}$, was above the long-term mean, $\tilde{\theta}$, a higher value of σ resulted in higher utility for the trader as the variance would change more rapidly. These results are consistent with those found in other areas of finance where stochastic volatility is concerned and the reader is referred to Yang (2010) for an analysis of option pricing under a Heston model.

We shall now shift our attention to the asymptotics of the problem given the considerable interest found in the multi-asset case. We will begin by examining the small-time-to-termination solution before extending to the perpetual problem and then finish will a large inventory analysis.

4.1 Small-time-to-termination solution ($\tilde{\tau} \to 0$)

To examine the small-$\tilde{\tau}$ solution we use the same perturbation method used in section 2.2. Substituting

$$f\left(\tilde{\tau}, q, \tilde{S}, \tilde{\nu}\right) = f_0\left(q, \tilde{S}, \tilde{\nu}\right) + \tilde{\tau} f_1\left(q, \tilde{S}, \tilde{\nu}\right) + \tilde{\tau}^2 f_2\left(q, \tilde{S}, \tilde{\nu}\right) + O\left(\tilde{\tau}^3\right), \tag{73}$$

into (64) we collect the $O\left(\tilde{\tau}^0\right)$ and $O\left(\tilde{\tau}^1\right)$ terms in which we find the values of $f_1\left(q, \tilde{S}, \tilde{\nu}\right)$ and $f_2\left(q, \tilde{S}, \tilde{\nu}\right)$ to be

$$f_1\left(q, \tilde{S}, \tilde{\nu}\right) = \left(-\tilde{\mu}\tilde{S}q + \frac{1}{2}\tilde{\nu}\tilde{S}^2 q^2 - \frac{\tilde{S}}{\tilde{S}+l}\left(\frac{l}{\tilde{S}+l}\right)^{\frac{l}{\tilde{S}}}\right) f_0\left(q, \tilde{S}\right), \tag{74}$$

and

$$\begin{aligned} f_2\left(q, \tilde{S}, \tilde{\nu}\right) = \frac{1}{2}\Bigg(&\tilde{\mu}\tilde{S} f_{1\tilde{S}} + \kappa\left(\tilde{\theta} - \tilde{\nu}\right) f_{1\tilde{\nu}} + \frac{1}{2}\tilde{\nu}\tilde{S}^2 f_{1\tilde{S}\tilde{S}} + \frac{1}{2}\sigma\tilde{\nu}^2 f_{1\tilde{\nu}\tilde{\nu}} + \rho\tilde{\nu}\sigma\tilde{S} f_{1\tilde{S}\tilde{\nu}} \\ &- \frac{1}{\tilde{S}+l}\left(\frac{l}{\tilde{S}+l}\right)^{\frac{l}{\tilde{S}}}\left(\left(l+\tilde{S}\right) f_1\left(q, \tilde{S}, \tilde{\nu}\right) - l f_1\left(q-1, \tilde{S}, \tilde{\nu}\right) e^{-\tilde{S}}\right)\Bigg), \end{aligned} \tag{75}$$

with f_0 given by the initial condition (65).

A comparison of the accuracy for the two-term and three-term asymptotic expansion can be seen in figure 14, in which we have shown a comparison for small $\tilde{S}$ (figure 14(a)) and larger $\tilde{S}$ (figure 14(b)). We examined these at a value of the variance, $\tilde{\nu}$, near the long term mean, $\tilde{\theta}$. It can be seen that the three-term asymptotic expansion is a strong approximation to the full numerical solution for $\tilde{\tau} \sim O(1)$. It is also worth noting that there are restrictions to how well the expansion approximates the full numerical solution. The larger we make the asset price, $\tilde{S}$, the faster the expansion deviates as an approximation for the full numerical solution. This is also the case as the variance, $\tilde{\nu}$, is increased.

4.2 The perpetual case ($\tilde{\tau} \to \infty$)

Let us now examine a perpetual type solution which was shown to be of asymptotical interest in the multiple-asset case and indeed the single asset case under constant volatility (see Blair et al., 2015). Assuming a steady-state, and thus setting

$$\frac{\partial f}{\partial \tilde{\tau}}\left(\tilde{\tau}, q, \tilde{S}, \tilde{\nu}\right) = 0 \quad \text{as} \quad \tilde{\tau} \to \infty,$$

the non-linear PDE (64) reduces to

$$\begin{aligned} &\tilde{\mu}\tilde{S} f_{\tilde{S}} + \frac{1}{2}\tilde{\nu}\tilde{S}^2 f_{\tilde{S}\tilde{S}} + \kappa\left(\tilde{\theta} - \tilde{\nu}\right) f_{\tilde{\nu}} + \frac{1}{2}\sigma^2\tilde{\nu} f_{\tilde{\nu}\tilde{\nu}} + \rho\sigma\tilde{\nu}\tilde{S} f_{\tilde{S}\tilde{\nu}} \\ &- \frac{e^l \tilde{S} f}{\tilde{S}+l}\left(\frac{l f\left(q, \tilde{S}, \tilde{\nu}\right)}{\left(\tilde{S}+l\right) f\left(q-1, \tilde{S}, \tilde{\nu}\right)}\right)^{\frac{l}{\tilde{S}}} = 0, \end{aligned} \tag{76}$$

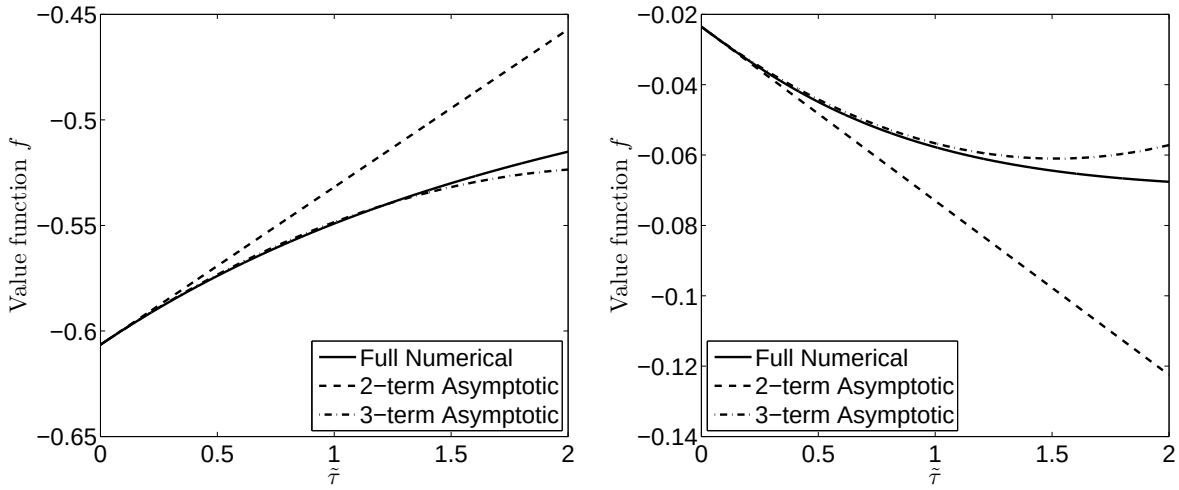

(a) $\tilde{S} = 0.5, \tilde{\nu} = 0.4$ (b) $\tilde{S} = 4, \tilde{\nu} = 0.4$

Figure 14: The above figures shows the comparison of the full numerical solution and the two-term and three-term asymptotical expansion of the value function, for $\tilde{S} = 0.5$ (figure 14(a)) and $\tilde{S} = 4$ (figure 14(b)). The parameter values used are $\tilde{\tau} = 2, l = 1, \tilde{\mu} = 0.05, \kappa = 0.75, \tilde{\theta} = 0.46, \sigma = 0.5$ and $\rho = -0.64$.

with $f = f\left(q, \tilde{S}, \tilde{\nu}\right)$ and initial condition (66). The optimal strategy for the steady-state solution takes the same form as (67).

To solve (76) we require two boundary conditions in each of the two semi-infinite domains of the asset price, $\tilde{S}$, and variance, $\tilde{\nu}$. These are analogous to the time-dependent case above, given by (68),(69),(71) and (72), but with the time derivative set to zero. We solve (76) using an iterative numerical method similar to that described in section 3. Figure 15 shows contour plots of the value function (figure 15(a)) and the optimal trading strategy (figure 15(b)). In figure 15(a) we can see the contours curve as the variance, $\tilde{\nu}$, increases indicating the value function is a decreasing function of $\tilde{\nu}$. This is resonated in figure 15(b), as we see the optimal trading strategy is a decreasing function of the variance, $\tilde{\nu}$.

4.2.1 Limit of small asset price $\left(\tilde{S} \to 0\right)$

Let us now consider the limit of (76) when the asset price is small, $\tilde{S} \to 0$, which previously has shown to give us insight into the parameter regimes to which solution exists. In the single asset case with constant volatility it was found that for a steady-state to exist the constraint

$$\tilde{\mu} < \frac{\tilde{\sigma}^2}{2}, \tag{77}$$

had to be satisfied, where $\tilde{\sigma}$ is the volatility of the GBM process driving the asset price, i.e. $\tilde{\nu}(\tau) = \tilde{\sigma}^2$ for all τ. This is not to be confused with σ, which is the volatility of the variance, $\tilde{\nu}(\tau)$. Given now we have stochastic volatility it is of interest to examine if similar constraints exist.

In the limit as $\tilde{S} \to 0$ asymptotic balancing suggests a solution of the form

$$f\left(q, \tilde{S}, \tilde{\nu}\right) = -1 + c(q)\,\tilde{S}^{\beta} e^{\alpha\tilde{\nu}}, \tag{78}$$

which solves the linear PDE

$$\tilde{\mu}\tilde{S} f_{\tilde{S}} + \frac{1}{2}\tilde{\nu}\tilde{S}^2 f_{\tilde{S}\tilde{S}} + \kappa\left(\tilde{\theta} - \tilde{\nu}\right) f_{\tilde{\nu}} + \frac{1}{2}\sigma^2\tilde{\nu} f_{\tilde{\nu}\tilde{\nu}} + \rho\sigma\tilde{\nu}\tilde{S} f_{\tilde{S}\tilde{\nu}} = 0, \tag{79}$$

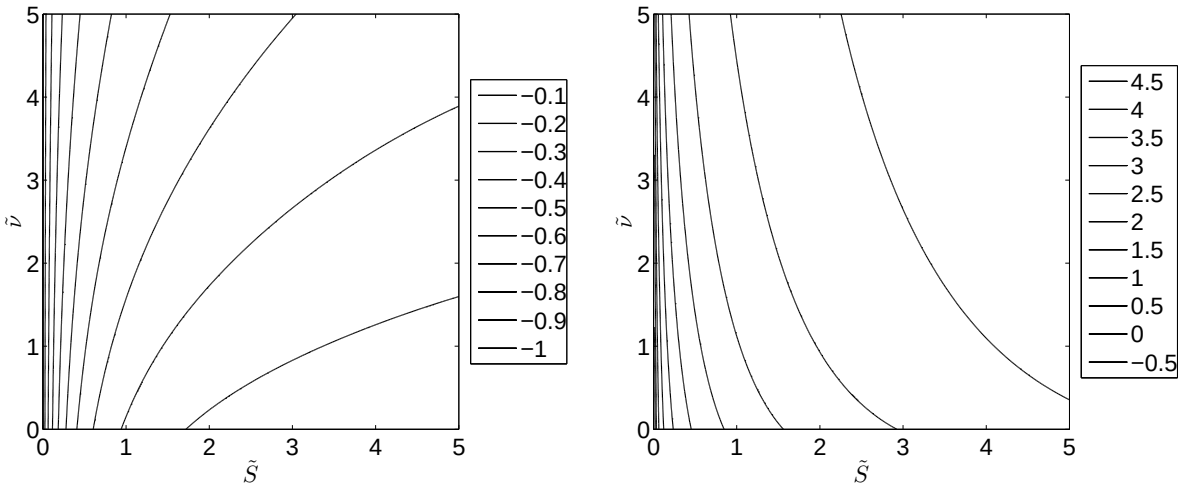

(a) Contour of f

(b) Contour of δ

Figure 15: Contour plot of stochastic volatility steady-state solution for value function (figure 15(a)) and optimal trading strategy (figure 15(b)). The parameter values used are $l = 1, \tilde{\mu} = 0.02, \kappa = 0.75, \tilde{\theta} = 0.46, \sigma = 2.78$ and $\rho = -0.64$.

with initial condition (66). Substituting (78) into (79) we obtain

$$\alpha = -\frac{\tilde{\mu}}{\kappa\tilde{\theta}}\beta \tag{80}$$

and

$$\frac{1}{2}\beta\left(\beta - 1\right) + \rho\sigma\beta\alpha + \frac{1}{2}\sigma^2\alpha^2 - \kappa\alpha = 0, \tag{81}$$

by collection the $O\left(\tilde{\nu}^0\right)$ and $O\left(\tilde{\nu}^1\right)$ terms respectively which when solved gives

$$\beta = \frac{\left(1 - \frac{2\tilde{\mu}}{\tilde{\theta}}\right)}{\left(1 - \frac{2\rho\sigma\tilde{\mu}}{\kappa\tilde{\theta}} + \left(\frac{\sigma\tilde{\mu}}{\kappa\tilde{\theta}}\right)^2\right)}, \tag{82}$$

which can be substituted into (80) to obtain α. For the solution to be bounded we need $\beta > 0$ and $\alpha < 0$. Firstly examining β we see that the denominator of (82) is always positive; this is clear when $\rho = 0$. At the extremes, when $\rho = \pm 1$ the denominator of (82) becomes

$$\left(1 \mp \left(\frac{\sigma\tilde{\mu}}{\kappa\tilde{\theta}}\right)\right)^2 > 0.$$

Therefore we have the constraint

$$\tilde{\mu} < \frac{\tilde{\theta}}{2}, \tag{83}$$

which is analogous to the constraint of the constant volatility case (77) given $\tilde{\theta}$ is the long-term mean of the variance. For $\beta > 0$ we need $\frac{\tilde{\mu}}{\kappa\tilde{\theta}} > 0$ for $\alpha < 0$ which sets the restriction

$$\tilde{\mu} > 0, \tag{84}$$

which is another parameter constraint. Figure 16 shows the comparison of the asymptotic solution given by (78), for small variance, $\tilde{\nu}$, (figure 16(a)) and larger variance (figure 16(b)). We can see the solution is approximated well in the small asset price, $\tilde{S}$, regime, before diverging away from the solution, for both small and larger variance, $\tilde{\nu}$.

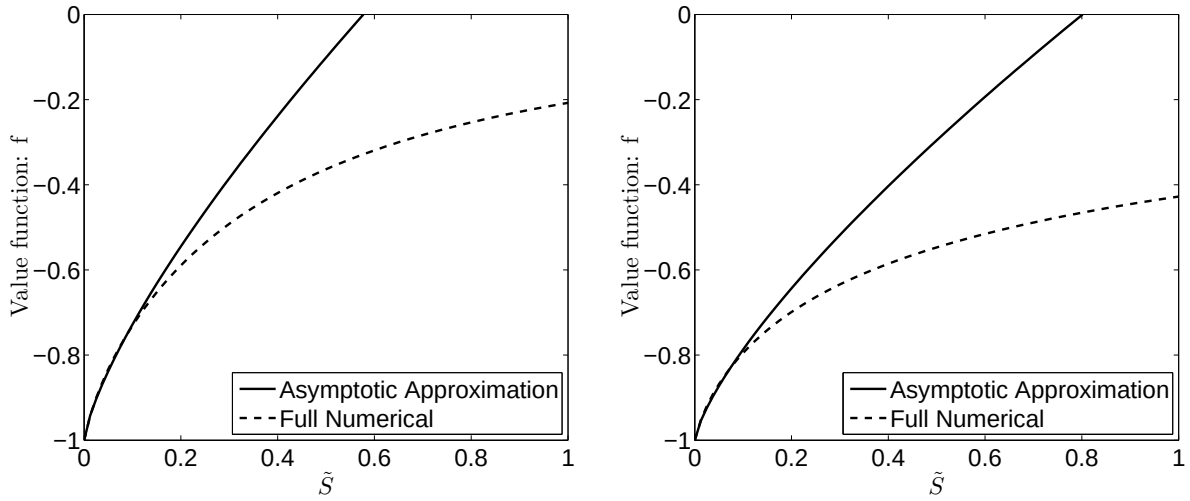

(a) $\tilde{\nu} = 0.25$ (b) $\tilde{\nu} = 4.00$

Figure 16: Above we compare the small $\tilde{S}$ asymptotical solution against the full numerical solution. We do this for small $\tilde{\nu}$ (figure 16(a)) and relatively large $\tilde{\nu}$ (figure 16(b)). We can see the solution is approximated well in the small $\tilde{S}$ regime, before diverging away from the solution, for both small and large $\tilde{\mu}$. The parameter values used are $l = 1, \tilde{\mu} = 0.02, \kappa = 0.75, \tilde{\theta} = 0.46, \sigma = 2.78$ and $\rho = -0.64$.

Given β mainly takes non-integer values, singular behaviour is present. In the small asset price limit, $\tilde{S} \to 0$, the optimal trading strategy is found, to leading order, to take the form

$$\delta^* \approx K(q)\, \tilde{S}^{\beta-1} e^{\alpha\tilde{\nu}}, \tag{85}$$

with $K(q) = \beta\left(c(q) - c(q-1)\right)$.

4.2.2 Large number of assets ($\tilde{q} \to \infty$)

We shall now investigate (briefly) the limit as the number of assets held becomes large, i.e. $q \to \infty$. It is found (confirmed by numerical investigation) that as $q \to \infty$

$$\lim_{q\to\infty} \frac{f\left(q, \tilde{S}, \tilde{\nu}\right)}{f\left(q-1, \tilde{S}, \tilde{\nu}\right)} \to 1, \tag{86}$$

which when substituted into (76) yields

$$\begin{aligned} &\tilde{\mu}\tilde{S} f_{\tilde{S}} + \frac{1}{2}\tilde{\nu}\tilde{S}^2 f_{\tilde{S}\tilde{S}} + \kappa\left(\tilde{\theta} - \tilde{\nu}\right) f_{\tilde{\nu}} + \frac{1}{2}\sigma^2\tilde{\nu} f_{\tilde{\nu}\tilde{\nu}} + \rho\sigma\tilde{\nu}\tilde{S} f_{\tilde{S}\tilde{\nu}} \\ &- \frac{e^l \tilde{S} f}{\tilde{S} + l}\left(\frac{l}{\left(\tilde{S} + l\right)}\right)^{\frac{l}{\tilde{S}}} = 0, \end{aligned} \tag{87}$$

with $f = f\left(\tilde{S}, \tilde{\nu}\right)$. This results in an optimal trading strategy which takes the form

$$\delta\left(\tilde{S}, \tilde{\nu}\right) = \frac{1}{\tilde{S}} \ln\left(\frac{\left(\tilde{S} + l\right)}{l}\right) - 1, \tag{88}$$

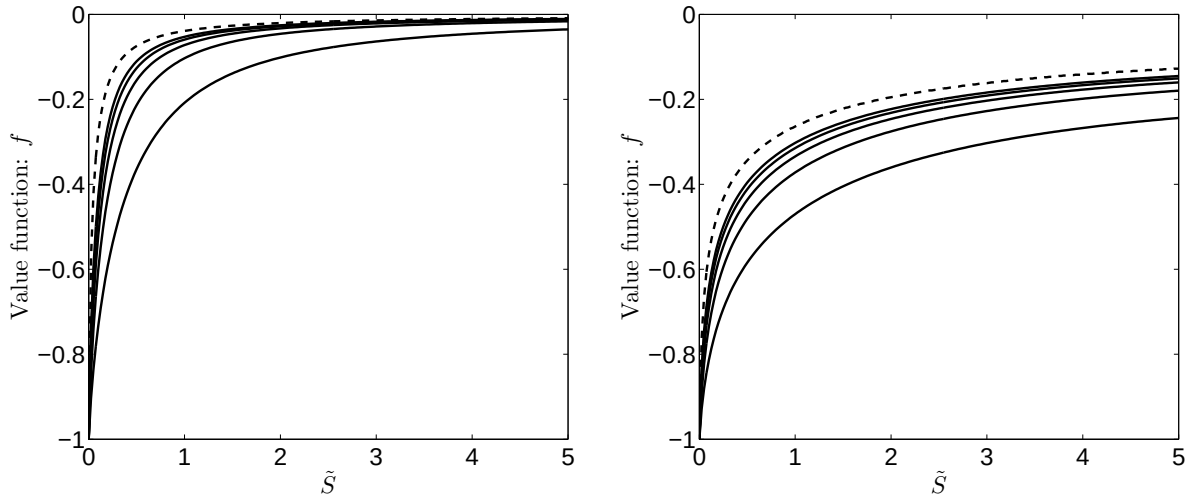

(a) $\tilde{\nu} = 0.25$ (b) $\tilde{\nu} = 5.00$

Figure 17: Above we compare the $q \to \infty$ solution against the solutions of increasing values of q. We plot $q = \{1, \ldots, 5\}$ which are represented by the increasing solid lines and converging to the $q \to \infty$ solution, represented by the broken line. We do this for small $\tilde{\nu}$ (figure 17(a)) and large $\tilde{\nu}$ (figure 17(b)). We can see the approximated is valid for small and large values of $\tilde{\nu}$, as well as all values in between. The parameter values used are $l = 1, \tilde{\mu} = 0.02, \kappa = 0.75, \tilde{\theta} = 0.46, \sigma = 2.78$ and $\rho = -0.64$.

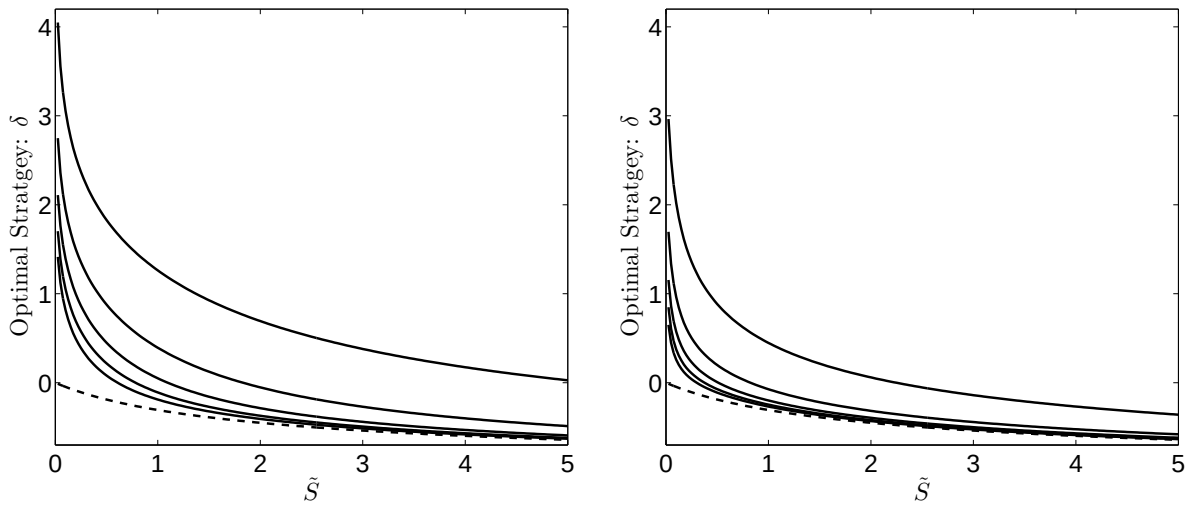

(a) $\tilde{\nu} = 0.25$ (b) $\tilde{\nu} = 5.00$

Figure 18: Above we compare the $q \to \infty$ solution against the solutions of increasing values of q for the optimal trading strategy, corresponding to those of figure 17. We plot $q = \{1, \ldots, 5\}$ which are represented by the increasing solid lines and converging towards the $q \to \infty$ solution, represented by the broken line. We do this for small $\tilde{\nu}$ (figure 18(a)) and relatively large $\tilde{\nu}$ (figure 18(b)). The parameter values used are $l = 1, \tilde{\mu} = 0.02, \kappa = 0.75, \tilde{\theta} = 0.46, \sigma = 2.78$ and $\rho = -0.64$.

which we notice is independent of the variance, $\tilde{\nu}$. Intuitively this makes sense, given that a trader with a large number of assets will receive a large amount of cash regardless of the asset price. The variance of the asset is thus not of concern to him.

To solve (87) we use a second-order finite difference scheme, implementing the same boundary conditions as used for the $q \sim O(1)$ case as discussed above in section 4.2. We examine the convergence of increasing the inventory, q, towards the large inventory, $q \to \infty$, solution. This can be seen in figure 17 for the value function and figure 18 for the optimal trading strategies. We have included two figures in each, one for small variance, $\tilde{\nu}$, and one for relatively large $\tilde{\nu}$. In each figure, we have curves representing increasing values of inventory, q, (solid curves) which converge towards the broken curve representing the large inventory, $q \to \infty$, solution. The values of the inventory we use are $q = \{1, \ldots, 5\}$. This convergence corroborates with our approximation of the ratio of the value function for subsequent inventory, q, values, given by (86).

5 Conclusion

In this paper we studied the optimal liquidation of a portfolio of correlated assets before examining the optimal liquidation of assets under a stochastic volatility framework. Both frameworks had previously been investigated for optimal liquidation using market orders (Almgren and Chriss framework), and our contributions extends that for optimal liquidation using limit orders. In both cases we used a dual approach of asymptotic and numerical methods to gain an insight of and understanding into the solution topology.

For the case of multiple assets we formulated the HJB PDE in a general sense of N assets before focusing on the two asset ($N = 2$) case. We were able to make a reduction in both the number of variables and input parameters (through non-dimensionalisation), as well as finding the optimal control in terms of the value function, thus drastically reducing the computation time needed to solve this problem. The numerical results were comparable with those found in MPT (see Markowitz, 1959). It was found that a trader with a portfolio of correlated assets traded in a way that resulted in a diversified portfolio, such as to minimise risk.

We examined a small-time-to-termination limit which has an analytic solution. This may be of use in a high-frequency trading framework where the time remaining is small and analytic solutions could be preferred over numerical solutions. In contrast, we examined a perpetual type solution in which the time-to-termination is large. For the perpetual problem we have investigated the small asset prices regime, $\tilde{S}_1, \tilde{S}_2 \to \infty$, using a change of variables to polar coordinate form. This gave insight into a parameter constraint as well as confirming singular behaviour which the numerical results were indicating. We also examined the limit as the number of assets held, q_1, q_2, was large, both together and separately.

We went on to study the liquidation of a portfolio of a single asset to which the volatility was governed by a Heston (1993) model. We again used a combined approach of accurate numerical methods and asymptotic analysis. Interesting trading strategies were found in comparison to the constant volatility case. For instance, if the variance was lower than the mean, the trader would trade faster when a quicker reversion to the mean was expected and trade slower if a slower reversion to the mean was expected. The opposite was true for variance above the long-term mean and indeed the properties of the solutions relate back to that of option pricing under stochastic volatility. Finally, given a parameter constraint was found in the constant volatility case for the perpetual problem (see Blair et al., 2015), we analysed the perpetual problem for the stochastic volatility model, with an interesting and comparable resultant outcome.

References

Alfonsi, A., Fruth, A., and Schied, A. (2010). Optimal execution strategies in limit order books with general shape functions. *Quantitative Finance*, 10(2):143–157.

Almgren, R. (2009). Optimal trading in a dynamic market. *Preprint*.

Almgren, R. (2012). Optimal trading with stochastic liquidity and volatility. *SIAM Journal on Financial Mathematics*, 3(1):163–181.

Almgren, R. and Chriss, N. (1999). Value under liquidation. *Risk*, 12(12):61–63.

Almgren, R. and Chriss, N. (2001). Optimal execution of portfolio transactions. *Journal of Risk*, 3:5–40.

Almgren, R. F. (2003). Optimal execution with nonlinear impact functions and trading-enhanced risk. *Applied Mathematical Finance*, 10(1):1–18.

Avellaneda, M. and Stoikov, S. (2008). High-frequency trading in a limit order book. *Quantitative Finance*, 8(3):217–224.

Bayraktar, E. and Ludkovski, M. (2012). Liquidation in limit order books with controlled intensity. *Mathematical Finance*.

Bellman, R. (1957). *Dynamical Programing*. Princton University Press.

Bertsimas, D., Lo, A. W., and Hummel, P. (1999). Optimal control of execution costs for portfolios. *Computing in Science and Engineering*, 1(6):40–53.

Black, F. (1976). Studies of stock price volatility changes. *Proceedings of the 1976 Meetings of the American Statistical Association*.

Blair, J., Johnson, P., and Duck, P. (2015). Analysis of optimal liquidation in limit order books. *Manchester Eprints*.

Brunetti, C., Kirilenko, A., and Mankad, S. (2011). Identifying high-frequency traders in electronic markets: Properties and forecasting.

Cartea, Á. and Jaimungal, S. (2013). Risk metrics and fine tuning of high-frequency trading strategies. *Mathematical Finance*.

Christie, A. A. (1987). On cross-sectional analysis in accounting research. *Journal of Accounting and Economics*, 9(3):231–258.

Cont, R. and De Larrard, A. (2013). Price dynamics in a markovian limit order market. *SIAM Journal on Financial Mathematics*, 4(1):1–25.

Cont, R., Stoikov, S., and Talreja, R. (2010). A stochastic model for order book dynamics. *Operations research*, 58(3):549–563.

Cox, J. C., Ingersoll Jr, J. E., and Ross, S. A. (1985). A theory of the term structure of interest rates. *Econometrica: Journal of the Econometric Society*, pages 385–407.

Cryer, C. W. (1971). The solution of a quadratic programming problem using systematic overrelaxation. *SIAM Journal on Control*, 9(3):385–392.

Duck, P. W., Evatt, G. W., and Johnson, P. V. (2014). Perpetual options on multiple underlyings. *Applied Mathematical Finance*, 21(2):174–200.

Engle, R. F. and Ng, V. K. (1993). Measuring and testing the impact of news on volatility. *The journal of finance*, 48(5):1749–1778.

Forsyth, P. A., Kennedy, J. S., Tse, S., and Windcliff, H. (2012). Optimal trade execution: a mean quadratic variation approach. *Journal of Economic Dynamics and Control*, 36(12):1971–1991.

Gabaix, X., Gopikrishnan, P., Plerou, V., and Stanley, H. E. (2006). Institutional investors and stock market volatility. *The Quarterly Journal of Economics*, 121(2):461–504.

Gopikrishnan, P., Plerou, V., Gabaix, X., and Stanley, H. E. (2000). Statistical properties of share volume traded in financial markets. *Physical Review E*, 62(4):R4493.

Guéant, O. and Lehalle, C.-A. (2013). General intensity shapes in optimal liquidation. *Mathematical Finance*.

Guéant, O., Lehalle, C.-A., and Fernandez-Tapia, J. (2012a). Dealing with the inventory risk: a solution to the market making problem. *Mathematics and Financial Economics*, pages 1–31.

Guéant, O., Lehalle, C.-A., and Fernandez-Tapia, J. (2012b). Optimal portfolio liquidation with limit orders. *SIAM Journal on Financial Mathematics*, 3(1):740–764.

Guilbaud, F., Mnif, M., and Pham, H. (2010). Numerical methods for an optimal order execution problem. *arXiv preprint arXiv:1006.0768*.

Heston, S. L. (1993). A closed-form solution for options with stochastic volatility with applications to bond and currency options. *Review of financial studies*, 6(2):327–343.

Ho, T. and Stoll, H. R. (1981). Optimal dealer pricing under transactions and return uncertainty. *Journal of Financial economics*, 9(1):47–73.

Kharroubi, I. and Pham, H. (2010). Optimal portfolio liquidation with execution cost and risk. *SIAM Journal on Financial Mathematics*, 1(1):897–931.

Markowitz, H. (1959). Portfolio selection: efficient diversification of investments. *New York*.

Maslov, S. and Mills, M. (2001). Price fluctuations from the order book perspective - empirical facts and a simple model. *Physica A: Statistical Mechanics and its Applications*, 299(1):234–246.

NAG (2014). *The NAG Library, The Numerical Algorithms Group (NAG), Oxford, United Kingdom*. www.nag.com.

Nelson, D. B. (1991). Conditional heteroskedasticity in asset returns: A new approach. *Econometrica: Journal of the Econometric Society*, pages 347–370.

Obizhaeva, A. A. and Wang, J. (2013). Optimal trading strategy and supply/demand dynamics. *Journal of Financial Markets*, 16(1):1–32.

Potters, M. and Bouchaud, J.-P. (2003). More statistical properties of order books and price impact. *Physica A: Statistical Mechanics and its Applications*, 324(1):133–140.

Press, W., Teukolsky, S., Vetterling, W., and Flannery, B. (2009). *Numerical recipes in C+: the art of scientific computing*. Cambridge University Press.

Schied, A. and Schöneborn, T. (2007). Optimal portfolio liquidation for cara investors. *Available at SSRN 1018088*.

Schied, A. and Schöneborn, T. (2009). Risk aversion and the dynamics of optimal liquidation strategies in illiquid markets. *Finance and Stochastics*, 13(2):181–204.

Schied, A., Schöneborn, T., and Tehranchi, M. (2010). Optimal basket liquidation for cara investors is deterministic. *Applied Mathematical Finance*, 17(6):471–489.

Schied, A. and Slynko, A. (2011). Some mathematical aspects of market impact modeling. *Available at SSRN 1735465.*

Smith, G. D. (1965). Numerical solution of partial differential equations.

Uhlenbeck, G. E. and Ornstein, L. S. (1930). On the theory of the brownian motion. *Physical review*, 36(5):823.

Weber, P. and Rosenow, B. (2005). Order book approach to price impact. *Quantitative Finance*, 5(4):357–364.

Wilmott, P. (1998). *Derivatives: The theory and practice of financial engineering.* Wiley Chichester.

Wilmott, P. (2007). *Paul Wilmott on Quantitative Finance, 3 Volume Set.* John Wiley & Sons.

Yang, C. (2010). *Multi-asset and stochastic volatility option and bond pricing models: valuations and calibrations.* PhD thesis, Doctoral thesis, School of Mathematics, University of Manchester, UK.